JOC The Journal of Organic Chemistry

Article

pubs.acs.org/joc

# β-Sheet-like Hydrogen Bonds Interlock the Helical Turns of a Photoswitchable Foldamer To Enhance the Binding and Release of Chloride

Semin Lee, Yuran Hua, and Amar H. Flood*

Chemistry Department, Indiana University, 800 East Kirkwood Avenue, Bloomington, Indiana 47405, United States

Supporting Information

**ABSTRACT:** Inspired by halorhodopsin's use of photoisomerization to regulate chloride, aryltriazole-based foldamers have been created to "catch and release" chloride ions upon light irradiation of end-appended azobenzenes. The proposed mode of stabilization exploits a β-sheet-like hydrogen-bonding array to cooperatively interlock the ends of a foldamer together with its helical core. We find that the hydrogen-bonding array has a greater influence on stabilizing the helix than the π-stacked seam under the conditions examined (50:50 MeCN/THF). Thus, we show how it is possible to enhance the difference between $Cl^-$ binding and release using light-dependent control over the foldamer's degree of helix stabilization. Making and breaking three π−π contacts with light caused an 8-fold change in chloride affinity (40 300 $M^{-1}$ ⇄ 5000 $M^{-1}$), five π−π contacts produced a 17-fold change (126 000 $M^{-1}$ ⇄ 7400 $M^{-1}$), and strategically located hydrogen-bonding units enabled a greater 84-fold differential (970 000 $M^{-1}$ ⇄ 11 600 $M^{-1}$). The improved performances were attributed to stepwise increases in the preorganization of the binding pocket that catches chloride while leaving the *cis* states with just one π−π contact relatively unchanged.

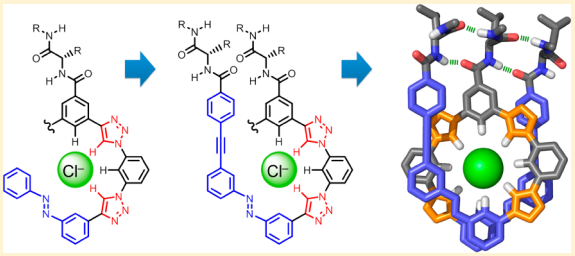


## INTRODUCTION

The controlled manipulation of ions is essential to biological[1] and chemical[2] processes. These include the selective transport of ions across membranes up and down concentration gradients using functional biomolecules.[3,4] In chemical systems, such as in phase-transfer catalysis[5,6] and during the safe handling of byproducts from the nuclear power industry, ions are usually manipulated using the principles of separation science.[7,8] While these applications have traditionally relied upon physical methods (e.g., liquid−liquid partitioning), they are now being used in conjunction with molecular receptors to confer unique selectivities (e.g., anion-induced asymmetric catalysis) or to enhance extraction (e.g., sulfate capture from nuclear wastes).[9] In order to introduce a means of control or to energize such systems, we[10] and others[11−13] are now investigating the use of ion receptors whose functions can be reversibly manipulated by light excitation. These synthetic designs take early inspiration from Shinkai's use of butterfly crowns[14,15] to regulate cations as much as from nature's proteins, such as photodriven halorhodopsin[16,17] that pumps chloride across membranes. Toward photoswitchable receptors for anions, we noted[18] from our formative study using a photoactive foldamer[10] (Figure 1) and from the photoactive receptors examined by others[19−23] that there is a limited change in the anion binding affinity upon switching, and little effort has been expended to date on improving their performance. We were therefore motivated to test whether cooperative contacts in the form of β-sheet-like formation of a hydrogen-bonding array could enhance the amount of chloride that is bound and released from the inside

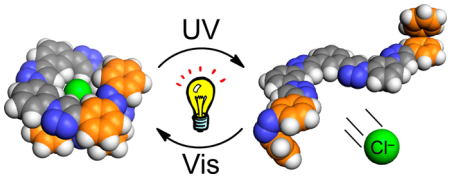


**Figure 1.** Illustration of binding and release of chloride by a light-active foldameric receptor.

of an aryltriazole cavity[24] formed from an azobenzene-appended foldamer.[25]

The photoactive foldamers examined here combine elements of foldameric receptors,[26] anion-induced folding,[27] solvophobic foldamers,[24,28] aryltriazole anion binding,[29−32] and azobenzene photoisomerism[33,34] into one chemically integrated system.[35] In the original photoactive foldamer **F0**,[10] its folded and helical *trans*−*trans* state (Figure 2 and Scheme 1) is stabilized by π stacking and directs four triazole CH donors toward the central cavity to form a competent chloride binding site ($K_a$ = 3000 $M^{-1}$, MeCN). UV-induced *trans*-to-*cis* photoisomerization of the two azobenzenes shortens the length of the foldamer's π−π-stacking surface[36] by an amount equivalent to two benzene rings. Therefore, the stability of the folded conformation decreases, and the position of its helix−random coil equilibrium shifts toward a less organized "random coil"

**Received:** July 31, 2014
**Published:** August 26, 2014

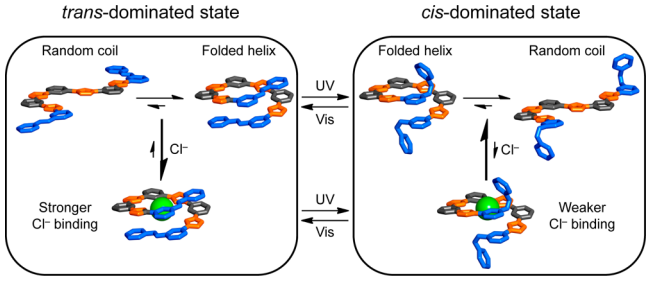


**Figure 2.** Idealized schematic of the pathways available for the binding and release of chloride from **F0** (the side chains and hydrogen atoms have been omitted for clarity). We offer only a thermodynamic view and cannot comment directly on the specific pathways followed.

with a concomitant reduction in the chloride binding affinity ($K_a$ = 380 $M^{-1}$, MeCN). This behavior was confirmed using variable-temperature studies of the circular dichroism (CD) response that arises when the L-leucine side chain induces a chiral preference in the helical backbone. Visible light is able to re-photoisomerize the foldamer back from the *cis*- to the *trans*-dominated state, largely restoring the chloride binding affinity. As a consequence, we made use of a 1:1 solution of **F0** and tetrabutylammonium chloride (TBACl) at 100 $\mu$M in MeCN to show that the free chloride concentration can be photoregulated between ∼55 and ∼20 $\mu$M, as reflected in the solution's electrical conductivity. However, we wondered whether it would be possible to enhance this differential by boosting the helical stability using orthogonal cooperative contacts.

Taking some inspiration from the structure of parallel $\beta$-sheets[37] (Figure 3), we introduced H-bonding contacts in a bid to better stabilize the helical form of the foldamer. In particular, we hypothesized that the two ends of the foldamer could be interlocked with the central rung of the helix by using the H-bonding donor−acceptor properties of the L-leucine and that this interlocking could be done cooperatively to enhance the helix's stability and thus its degree of organization toward $Cl^-$ binding. With the aid of molecular modeling, we designed foldamer **F3** in which modified L-leucines were incorporated into the two ends of the foldamer and in which phenylacetylenes were believed to provide sufficient length extension to allow the array of H-bonds to form. Thus, we created the series of foldamers **F1**, **F2**, and **F3** (Scheme 1) as a means to identify the role of the extended $\pi$−$\pi$-stacking surfaces (**F1** vs **F2**) and then to distinguish their effect from the H-bonding interlocks (**F2** vs **F3**). While combinations of $\pi$ stacks and H-bonds have been investigated previously with modified helical peptides[38] and in abiological indolocarbazole foldamers,[39] this may be one of the first times that their respective contributions to cooperativity have been distinguished from each other. Furthermore, even though we showed early on that triazoles can also bind metal cations,[40] they do so weakly. Involvement of the counter cation has been studied extensively[29d,e] through the use of multiple titrations conducted at multiple concentrations and analyzed using complementary approaches to unravel the presence and impact of ion pairing. For this reason, the noncoordinating $TBA^+$ cation was used in conjunction with polar "dissociating" solvents to greatly reduce the number of equilibria present in solution down to the elementary 1:1 binding process of foldamer plus chloride.

We show that the differences between the chloride affinities of the *trans* and *cis* forms of the photoactive foldamers display an increase across the series **F1** → **F3** (Figure 4). Using solvophobic principles and CD spectroscopy, we find that the cooperative contacts increasingly enhance the thermal stability of the foldamers when the two azobenzenes are in their *trans* form. Conversely, we show that photoisomerization of one and then two azobenzenes into their *cis* forms halve (*cis*−*trans*) and then largely extinguish (*cis*−*cis*) these cooperative non-covalent contacts, respectively. Across the series **F1** → **F3**, therefore, the foldamers show increasingly stable helices and, upon light irradiation, switch into similarly disorganized random coils. Using electrical conductivity measurements of TBACl salt solutions (20 $\mu$M) bearing each foldamer (20 $\mu$M), we demonstrate that the concentrations of chloride present in solution can be modulated reversibly between low and high

**Scheme 1. Light-Active Foldamers F0,[10] F1, F2, and F3**

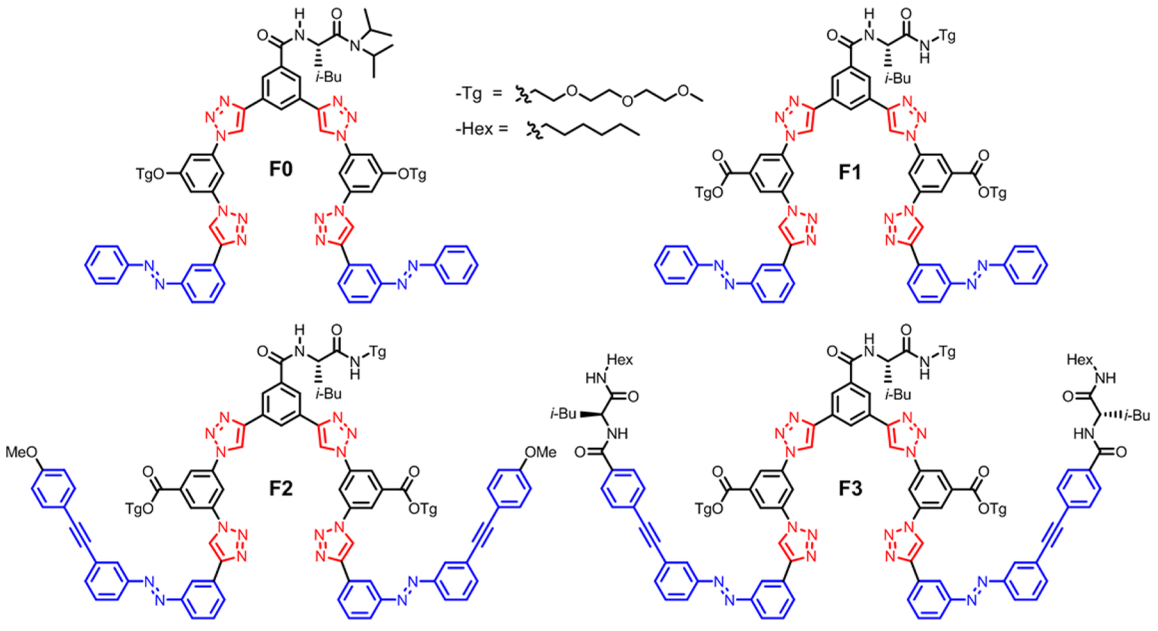



dx.doi.org/10.1021/jo501595k | J. Org. Chem. 2014, 79, 8383−8396

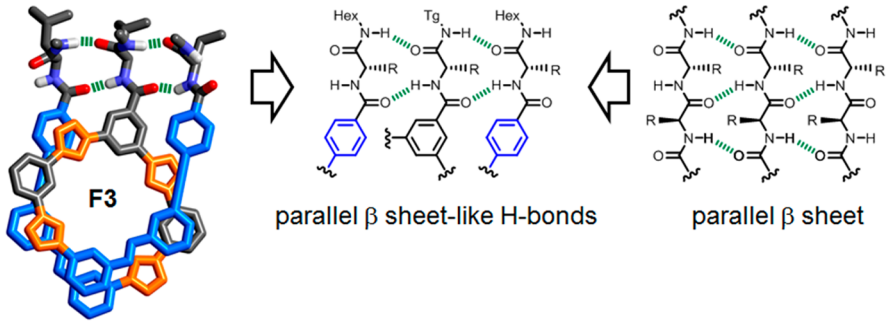


**Figure 3.** Illustratation of the structure of **F3** with parallel $\beta$-sheet-like H-bonded amino acid side chains.

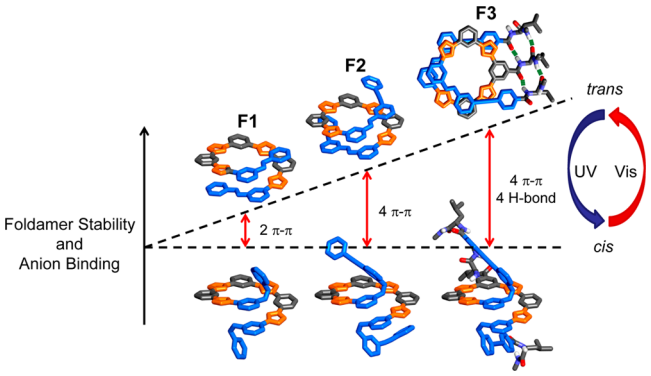


**Figure 4.** Hypothesized energy diagram of foldamers **F1**, **F2**, and **F3** in idealized conformations for chloride binding (triazole units are highlighted in red and photoactive units in blue).

values using UV and visible-light irradiation: **F1** (15−18 $\mu$M), **F2** (12−17 $\mu$M), and **F3** (8−16 $\mu$M). Taken all together, these series of experiments indicate that stimuli-dependent modulation of the foldamer's stability can be used to conformationally regulate the chloride binding site and in turn to provide a means to control the availability of free chloride ions.

## RESULTS AND DISCUSSION

**Syntheses of Light-Active Foldamers.** The design of **F1**−**F3** is based on the parent foldamer **F0**.[10] For practical reasons, however, the structure of **F0** was modified to generate the structure of **F1** (Scheme 1), which also serves as the core of foldamers **F2** and **F3**. Consequently, all of the receptor cavities present the same number of CH hydrogen-bond donors. First, triethylene glycol (Tg) was employed as a substituent on the central L-leucine to provide broader solubility. Second, the Tg side chains present on the phenylene linkers located east and west were introduced using esters in **F1** to provide easier syntheses.[30f] The esters also serve as electron-withdrawing groups to enhance the strength of both the phenylene CH···$Cl^-$ hydrogen bonds[41] and any $\pi$−$\pi$ stacking.[42]

Foldamers **F1**, **F2**, and **F3** were synthesized from their components by stitching together the appropriate subunits using a series of Sonogashira cross-coupling[43] and copper(I)-catalyzed azide−alkyne cycloaddition (CuAAC) reactions.[44] Building block **4** was used as the central component of each foldamer. Amide coupling between *tert*-butylcarbamate (Boc)-protected L-leucine (**1**) and 2-(2-(2-methoxyethoxy)ethoxy)-ethanamine followed by Boc group deprotection provided **2** (Scheme 2). Compound **2** was then coupled with 3,5-diiodobenzoic acid to give diiodo compound **3**. The central building block **4** was synthesized by Sonogashira coupling of **3** with trimethylsilylacetylene (TMSA) followed by desilylation. Preparation of the foldamer's arms proceeded with a click reaction between 3-ethynylazobenzene (**5**) and an excess amount of diazidobenzene **6**[45] to yield monoazido building

**Scheme 2. Synthesis of F1**[a]

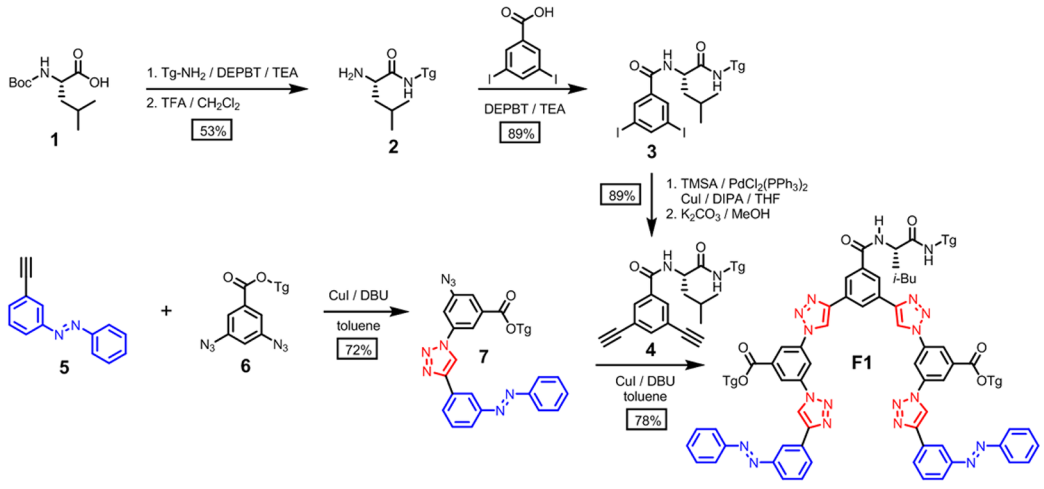


[a]Abbreviations: DEPBT, 3-(diethoxyphosphoryloxy)-1,2,3-benzotrazin-4(3*H*)-one; TEA, triethylamine; DBU, 1,8-diazabicyclo[5.4.0]undec-7-ene; DIPA, diisopropylamine; TMSA, trimethylsilylacetylene.


dx.doi.org/10.1021/jo501595k | J. Org. Chem. 2014, 79, 8383−8396

**Scheme 3. Synthesis of $\pi$-Extended F2**

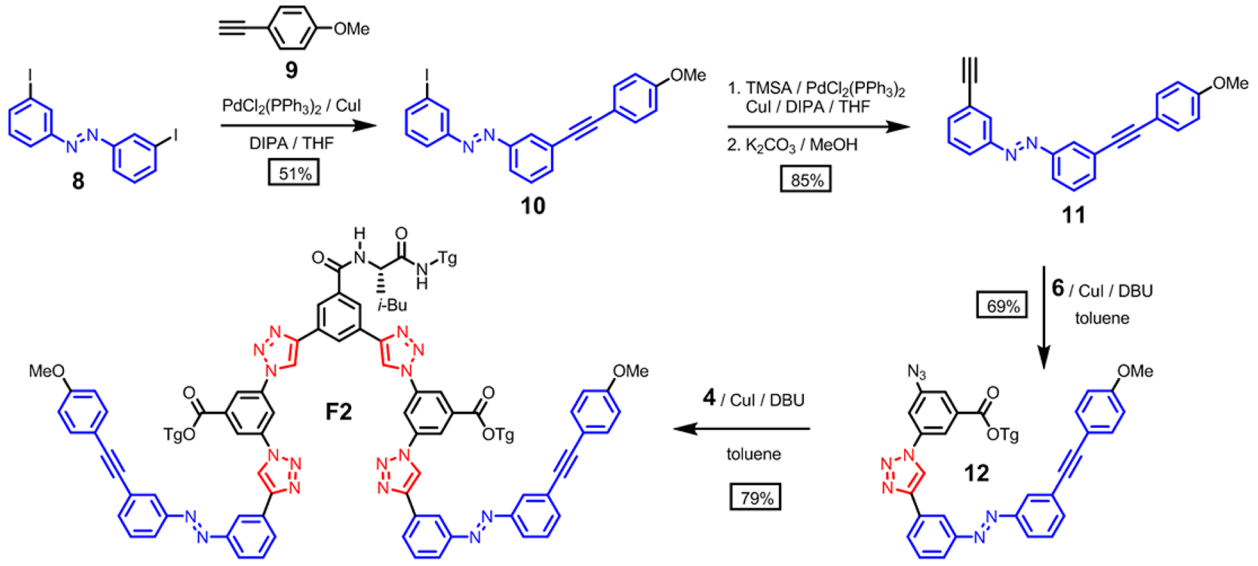


**Scheme 4. Synthesis of F3 via a Series of Sonogashira Coupling and CuAAC Reactions**

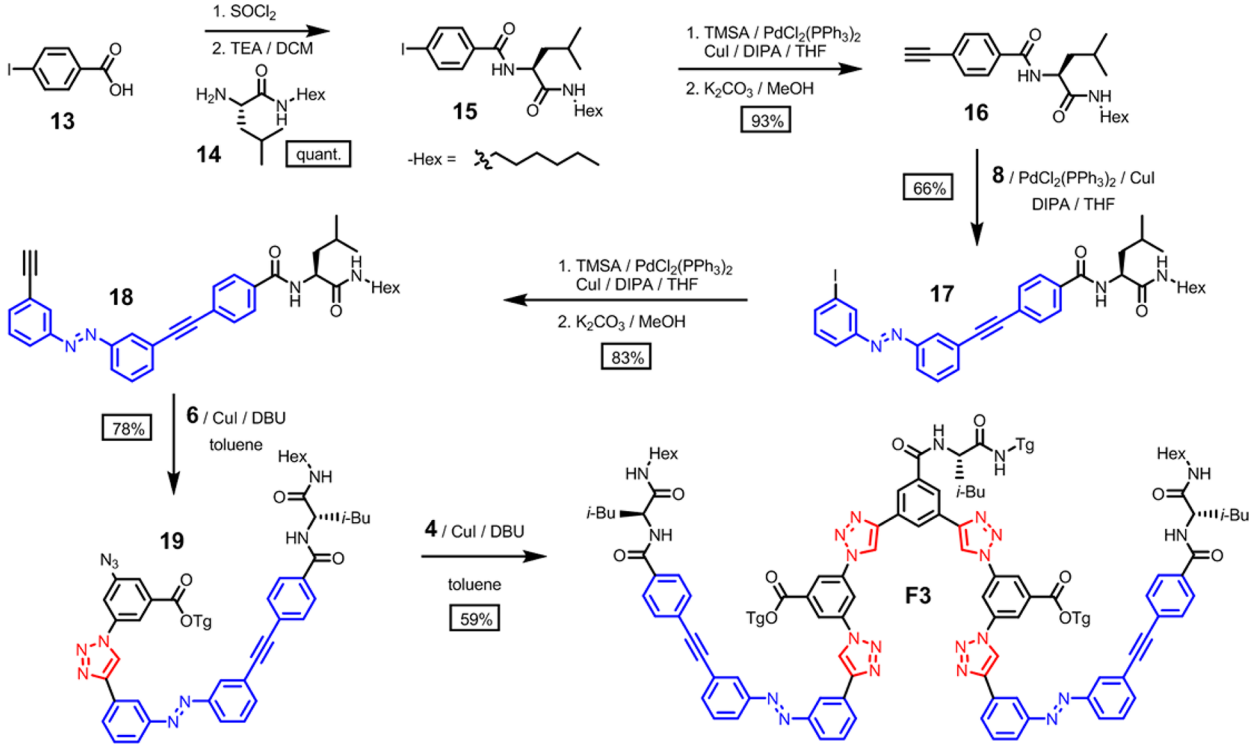


block **7**. The final CuAAC reaction between central building block **4** and monoazido arms **7** provided **F1**.

The preparation of **F2** followed a strategy similar to that for **F1** (Scheme 3). The longer arms **10** were created by Sonogashira coupling of *p*-ethynylmethoxybenzene (**9**)[46] with an excess amount of 3,3′-diiodoazobenzene (**8**).[47] Compound **10** was subjected to Sonogashira coupling with TMSA, and subsequent desilylation to yield 3-ethynylazobenzene analogue **11** bearing a phenylacetylene group. Performing a CuAAC reaction on this compound with an excess of **6** gave mono(azido)azobenzene building block **12**. The long foldamer **F2** was synthesized by a final CuAAC reaction between the central diethynylphenylene **4** and azobenzene building block **12**.

The preparation of H-bonded foldamer **F3** (Scheme 4) started with the functionalization of the terminal phenyl arms. *p*-Iodobenzoic acid (**13**) was converted to an acyl chloride derivative, which was then reacted with L-leucine derivative **14** (see the Supporting Information) to give iodobenzamide compound **15**. Sonogashira coupling of **15** with TMSA followed by desilylation provided ethylnylbenzamide **16**. Compound **16** was coupled with excess **8** to yield leucine-functionalized iodoazobenzene **17**, which was subjected to Sonogashira coupling with TMSA followed by desilylation to provide ethynylazobenzene derivative **18**. Monoazido building


dx.doi.org/10.1021/jo501595k | J. Org. Chem. 2014, 79, 8383−8396

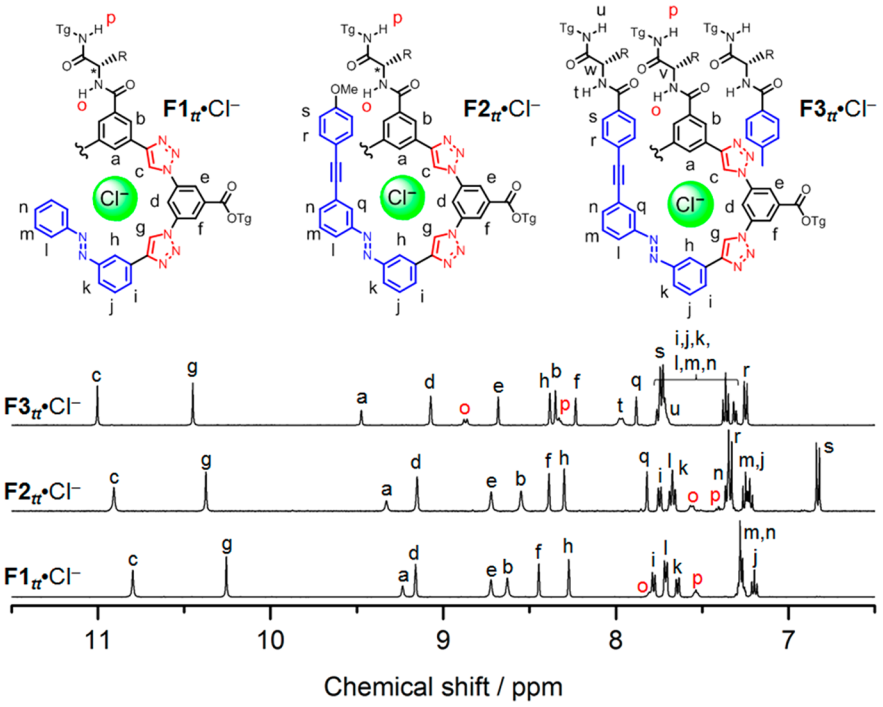


**Figure 5.** $^1$H NMR spectra of $\mathbf{F1}_{tt}$, $\mathbf{F2}_{tt}$, and $\mathbf{F3}_{tt}$ with 10 equiv of TBACl (5 mM, $CD_2Cl_2$, 500 MHz).

block **19** was obtained by reacting **18** with excess diazidobenzene **6** under CuAAC conditions. Finally, a click reaction between diethynylphenylene **4** and side arm **19** finally provided **F3**. All of the compounds were characterized by $^1$H and $^{13}$C NMR spectroscopy and mass spectrometry.

**Definition of Photostationary States and Photoisomers.** Foldamers **F0**, **F1**, **F2**, and **F3** each have two azobenzenes, allowing access to three possible photoisomers: *trans*–*trans* ($\mathbf{F}_{tt}$), *cis*–*trans* ($\mathbf{F}_{ct}$) and *cis*–*cis* ($\mathbf{F}_{cc}$). The as-prepared foldamers are initially in their thermally stable *trans*–*trans* states ($\mathbf{F}_{tt}$). Azobenzenes are not able to photoisomerize perfectly between *trans* and *cis*, with 80% conversion in either direction being typical.[48] Therefore, the UV-photostationary states (**F-UV**) accessed by UV irradiation (365 nm) and the visible-photostationary states (**F-Vis**) accessed by visible-light irradiation (436 nm) are mixtures of the $\mathbf{F}_{cc}$, $\mathbf{F}_{ct}$, and $\mathbf{F}_{tt}$ photoisomers in different ratios. These photostationary state (PSS) distributions were measured and incorporated in the analyses that follow.

**Solvent Conditions Affecting Helical Stability and Solubility.** Polar solvents direct nonpolar foldamers to fold in a solvophobic manner, and nonpolar solvents drive them toward random coils.[49] Consequently, the selection of solvents was crucial for investigating the properties of **F1**, **F2**, and **F3**. For this reason, MeCN ($\varepsilon$ = 36.6) was selected as the poor solvent capable of inducing helical folding. At the same time, however, MeCN reduced the solubilities of **F2** and **F3** (with their extended hydrophobic $\pi$ surfaces) compared with **F1**. THF ($\varepsilon$ = 7.5) was found to be a good solvent that both unfolded and solubilized the foldamers. Therefore, a 50% MeCN/THF mixture was found to balance folding with retention of a homogeneous solution free from aggregation. Homogeneity was also dependent on concentration: CD spectroscopy conducted on **F3** identified the emergence of aggregates at 10 $\mu$M but not at 4 $\mu$M (see the Supporting Information). Consequently, the chloride binding energy was determined in 50% MeCN/THF at 4 $\mu$M for H-bonded foldamer **F3**. In 50% MeCN/THF, neither **F1** nor **F2** displayed a CD response, consistent with negligible folding. Increasing the MeCN content induced more folding in **F1** and **F2**, allowing the two of them to be compared using variable-temperature (VT) CD spectroscopy.

**$^1$H NMR Characterization of the Foldamers.** The $^1$H NMR spectra of foldamers **F1**, **F2**, and **F3** were recorded in $CD_2Cl_2$ to aid in their structural analysis by comparison to prior studies.[10,29] Quantitative studies were conducted in the solvents in which the light-driven experiments of binding and release were evaluated in order to provide a quantitative understanding of the regulation of the chloride concentrations. Spectra of the foldamers alone showed broad aromatic signals characteristic of conformational dynamics (see the Supporting Information). Consequently, 10 equiv of TBACl was added to each sample to obtain sharp, resolved peaks (Figure 5). Final assignments were also made with the aid of through-bond $^1$H correlation spectroscopy (COSY) and through-space $^1$H nuclear Overhauser effect spectroscopy (NOESY) experiments, as detailed in the Supporting Information.

The $^1$H NMR spectra of **F1**, **F2**, and **F3** (Figure 5) provide evidence for structural distinctions among the foldamers. The two NH proton signals originating from leucine on the central phenylene ($H^o$, $H^p$) in both **F1** and **F2** are situated below 8 ppm. On the other hand, **F3** has both of these signals noticeably shifted to above 8 ppm, which is indicative of the desired formation of H-bonds between the three leucine groups of the helically folded structure. In addition, the $J_{NH-HC^*}$ coupling constants for $H^o$ with $H^v$ (9.0 Hz) and $H^t$ with $H^w$ (8.5 Hz) are consistent with a geometry that resembles $\beta$-sheets in peptides.[37] Phenylene protons $H^a$ and triazole protons $H^c$ and $H^g$, which form the inner binding pockets, exist at the most downfield positions as a result of CH···anion H-bonding.[10,29,50] The positions of these proton resonances suggest that chloride affinities increase along the series (i.e., **F1** < **F2** < **F3**).[30f]


dx.doi.org/10.1021/jo501595k | J. Org. Chem. 2014, 79, 8383–8396

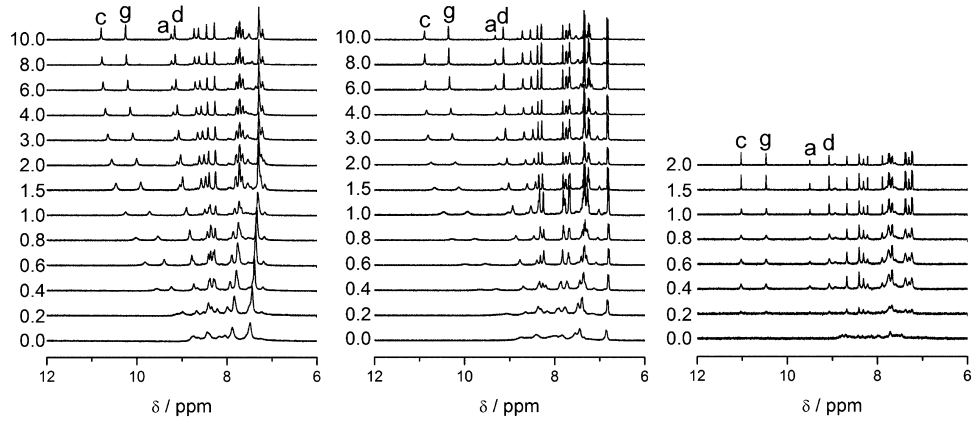


**Figure 6.** $^1$H NMR spectra showing titrations of TBACl with (left) **F1**$_{tt}$, (center) **F2**$_{tt}$, and (right) **F3**$_{tt}$ (5 mM, $CD_2Cl_2$, 298 K, 500 MHz).

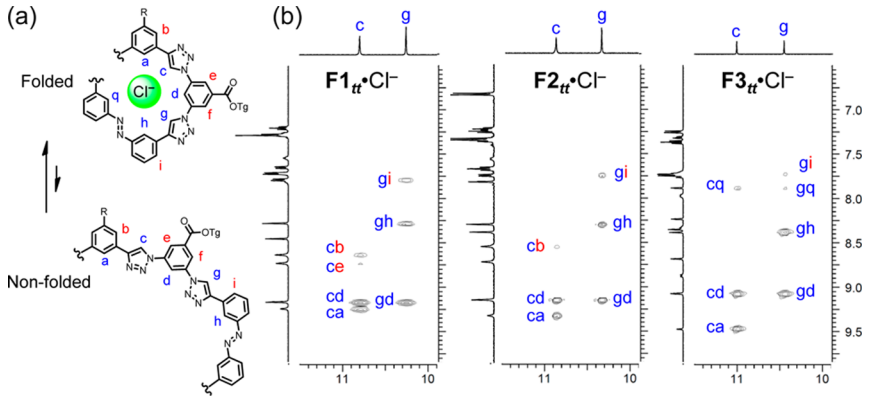


**Figure 7.** (a) Representative structures of the folded conformation and one of the possible nonfolded conformations. (b) Partial 2D NOESY spectra of **F1**, **F2**, and **F3** with 10 equiv of TBACl (5 mM, $CD_2Cl_2$, 500 MHz, 25 °C, mixing time = 0.8 s).

Interestingly, H$^d$, which is also proximal to the bound chloride, moved more upfield across this series, presumably as a result of increased $\pi-\pi$-stacking interactions involving foldable arms.

**NMR Titrations with Chloride.** NMR titrations of foldamers **F1**$_{tt}$, **F2**$_{tt}$, and **F3**$_{tt}$ with TBACl in $CD_2Cl_2$ (Figure 6) revealed the strength and time scale of the chloride binding process. Upon addition of TBACl, the aromatic peaks of **F1**$_{tt}$ and **F2**$_{tt}$ sharpened and showed continual shifts consistent with fast exchange on the NMR time scale. The protons that form the chloride binding cavity (H$^g$, H$^c$, H$^a$, and H$^d$) all exhibited gradual downfield shifts that reached saturation at different equivalence points. Foldamer **F1**$_{tt}$ became saturated with 6−10 equiv of chloride, while **F2**$_{tt}$ reached saturation after the addition of 3−4 equiv.[29b] By contrast, **F3**$_{tt}$ displayed sharp peaks that grew into their downfield positions, indicative of slow exchange on the NMR time scale, and the end point occurred upon the addition of 1−2 equiv of chloride, consistent with the tightest binding among the three foldamers.

**Secondary Structures of the Foldamers.** The secondary structures of **F1**, **F2**, and **F3** were determined with the aid of NOESY $^1$H NMR spectroscopy (Figure 7) recorded in the presence of 10 equiv of TBACl in $CD_2Cl_2$. All of the spectra exhibited strong cross-peaks between the inner protons that line the binding site (H$^{c-a}$, H$^{c-d}$, H$^{g-d}$, H$^{g-h}$) and a medium cross-peak between the triazole protons (H$^{c-g}$). The cross-peaks corresponding to the nonfolded conformations (H$^{c-e}$, H$^{c-b}$, H$^{g-f}$, H$^{g-i}$) were weaker. Thus, all three foldamers show a preference for the folded state when the chloride is bound. **F3** exhibited additional 2D NOESY cross-peaks (see the Supporting Information) that provided further insight into the folded conformation in the presence of 10 equiv of TBACl. The triazole proton H$^c$ showed through-space connections to H$^r$ and H$^q$ from the phenylethynylene unit stacked directly on top of it (Figure 8). Similarly, the H$^{b-s}$, H$^{b-r}$, and H$^{d-q}$ cross-peaks between stacking phenylene groups are consistent with the helically folded structure. Taken together with the *J*-coupling data (vide supra) and the downfield-shifted positions involving the leucine groups, the model (Figure 8) largely reflects the initial design (Figure 3) in which the helix is interlocked with $\beta$-sheet-like H-bonding.

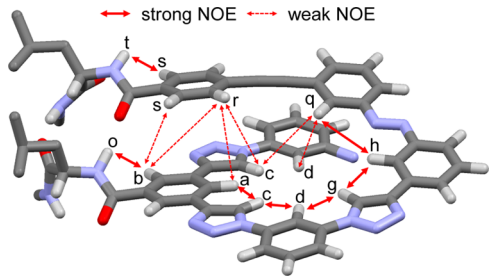


**Figure 8.** Partial structure of a model of **F3** in the presence of 10 equiv of TBACl in $CD_2Cl_2$ (5 mM, 500 MHz, 25 °C, mixing time = 0.8 s). The structure was minimized with molecular mechanics. Representative NOESY cross-peaks are shown.

**NMR Studies of Photoisomerization.** The degree of photoisomerization to the *cis*-dominated state (UV light)


dx.doi.org/10.1021/jo501595k | J. Org. Chem. 2014, 79, 8383−8396

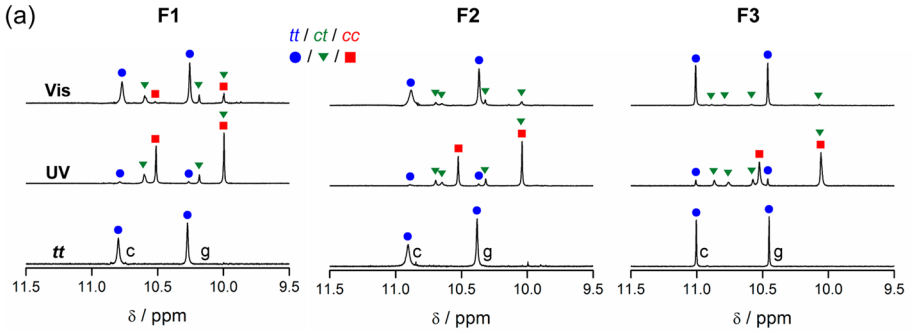


(b)

| F1 | tt | ct | cc |
|---|---|---|---|
| Vis | 75 | 22 | 3 |
| UV | 5 | 32 | 63 |

| F2 | tt | ct | cc |
|---|---|---|---|
| Vis | 83 | 17 | 0 |
| UV | 5 | 32 | 63 |

| F3 | tt | ct | cc |
|---|---|---|---|
| Vis | 94 | 6 | 0 |
| UV | 8 | 28 | 64 |

**Figure 9.** (a) $^1$H NMR spectra of **F1**, **F2**, and **F3** with 10 equiv of TBACl (5 mM, $CD_2Cl_2$, 500 MHz) before irradiation and after UV and visible-light irradiation. (b) Ratios of photoisomers calculated by peak integration.

largely followed statistical populations, while photoisomerization to the *trans*-dominated states (visible light) featured the assistance of non-covalent contacts. $^1$H NMR spectra of **F1**, **F2**, and **F3** in the presence of 10 equiv of TBACl were recorded after UV (365 nm) and visible-light (436 nm) irradiation (Figure 9a). The populations of the *tt*, *ct*, and *cc* species in each of the UV and visible photostationary states were calculated using integration values of two triazole proton peaks, $H^c$ and $H^g$ (Figure 9b).

The UV photostationary states for foldamers **F1**, **F2**, and **F3** had a *tt*:*ct*:*cc* ratio close to the statistical ratio of 4:32:64 (considering that the UV PSS of a typical azobenzene unit has a *trans*-to-*cis* photoisomerization efficiency of 80%). On the other hand, the ratio of the *tt* isomer in the visible photostationary state increased across the series **F1** → **F3**, with a concomitant decrease in the two *cis*-dominated isomers; the *ct* isomer ratio fell to 6% and the population of the *cc* isomer eventually dropped below the detection limit of the $^1$H NMR experiment for **F3** (Figure 9b). On the basis of these ratios, the *cis*-to-*trans* photoisomerization efficiencies for the individual azobenzenes were deconvoluted to be 86%, 91%, and 97% for **F1**, **F2**, and **F3**, respectively. It can be postulated that the formation of the foldamer–chloride complexes affects the relative stability of the isomers in the visible PSS.[51] Similar behavior was observed by Shinkai,[14,15] where a butterfly-like crown ether compound had a photostationary state with higher *cis* ratios when binding larger cations to achieve greater stabilities for the clam-shell complexes.

**Foldamer Stabilities Measured Using Circular Dichroism.** The helix-forming propensities of the foldamers increase in the order **F1** < **F2** < **F3**, as verified using CD spectroscopy. It was expected that the foldamers would fold in the presence of polar solvents. Consistently, **F3** folded upon addition of 50% MeCN in THF (see the Supporting Information), whereas **F1** and **F2** required greater fractions of MeCN. Consequently, increasing the volume fraction of MeCN in THF led to an increase in the negative CD signals ($\Delta\varepsilon$ = difference in molar extinction coefficient) throughout the UV region (250–350 nm) for $\mathbf{F1}_{tt}$ and $\mathbf{F2}_{tt}$ (Figure 10a,b), characteristic of solvophobic helical foldamers.[10] The CD response at or below 250 nm was assigned to the intrinsic response of the chiral amino acid side group on the basis of similar observations obtained from a nonfoldameric oligomer (**20**; see the Supporting Information). Tracking the CD signal observed at

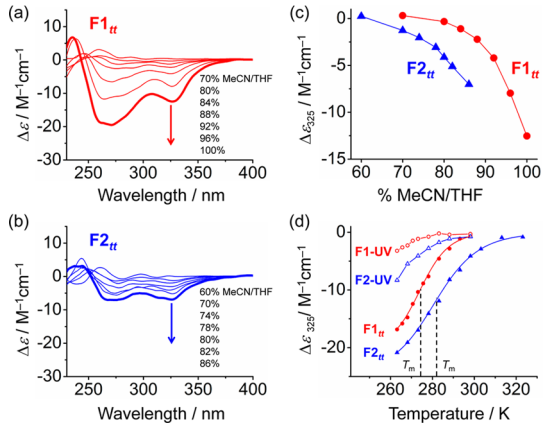


**Figure 10.** (a, b) Solvent-dependent CD spectra of (a) $\mathbf{F1}_{tt}$ and (b) $\mathbf{F2}_{tt}$ (20 $\mu$M, 25 °C). (c) CD response ($\Delta\varepsilon$) observed at 325 nm for $\mathbf{F1}_{tt}$ and $\mathbf{F2}_{tt}$ as a function of MeCN volume fraction. (d) Variable-temperature CD responses of **F1** and **F2** observed at 325 nm (20 $\mu$M in 80% MeCN/THF) for the *trans*–*trans* isomers (with fitting curves) and for the UV photostationary states.

325 nm (Figure 10c) showed that $\mathbf{F2}_{tt}$ starts folding with less MeCN, consistent with helix's greater stability relative to $\mathbf{F1}_{tt}$.

The helical stability of the folded state of **F2** is greater than that of **F1**, and both were lowered upon UV photoirradiation to their *cis*-dominated states. Melting curves (Figure 10d) were generated by measuring the CD response ($\Delta\varepsilon$) at 325 nm as a function of temperature, and all showed a sigmoidal response, indicating that the melting is cooperative. The melting temperatures ($T_m$) of $\mathbf{F1}_{tt}$ and $\mathbf{F2}_{tt}$ were determined by fitting the data points between 270 and 340 nm to a two-state thermal unfolding model[52] (see the Supporting Information). The corresponding $T_m$ obtained for $\mathbf{F2}_{tt}$ (8.1 ± 0.4 °C) was higher than that for $\mathbf{F1}_{tt}$ (1.0 ± 0.2 °C), which is consistent with the hypothesis that the increased chain length of foldamer **F2** provides greater thermal stability for the helix.[10] Upon UV (365 nm) irradiation to convert from the *trans*–*trans* states to the *cis*-dominated photostationary states **F1-UV** and **F2-UV**, the CD signals decreased, consistent with increased ratios of random-coil conformations. The melting curves show lower melting temperatures and reduced thermal stabilities compared with the *trans*–*trans* states. However, full sigmoidal curves were not obtained for **F1-UV** and **F2-UV** across the temperature range


dx.doi.org/10.1021/jo501595k | J. Org. Chem. 2014, 79, 8383–8396

examined (down to −10 °C) which precluded a closer examination of the differential stabilization. Nevertheless, it is clear that **F2-UV** is more stable than **F1-UV**. This difference arises from the nature of the UV photostationary states. On the basis of our model, we expect the *cis*−*cis* isomers to have similar stabilities with just one $\pi-\pi$ contact each. However, the 32% *cis*−*trans* and 5% *trans*−*trans* isomers present after UV photoisomerization contribute to the greater thermal stability of **F2-UV** over **F1-UV**.

The solvent dependence of the CD spectra of **F3** (Figure 11) showed very different characteristics compared with those of **F1**

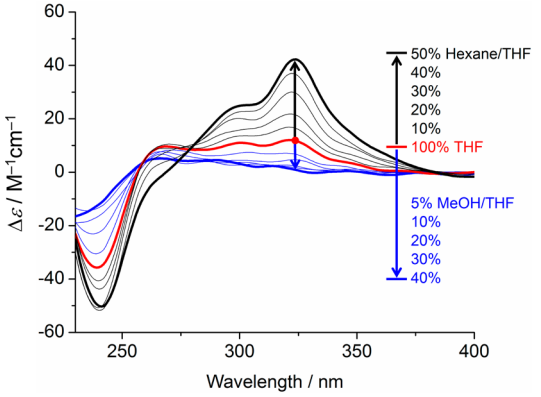


**Figure 11.** Solvent-dependent CD spectra of $\mathbf{F3}_{tt}$ (5 $\mu$M) at 25 °C.

and **F2**. **F3** has a positive signal in the 270−400 nm region in the CD spectrum recorded under the same solution conditions (see the Supporting Information), indicating an opposite helicity from **F1** and **F2**. The amino acid region below 250 nm is inverted, indicating that the means of chiral induction likely differ for the two classes of foldamers. Solvent-dependent ellipticities recorded using 10−50% MeCN in THF showed negligible changes (see the Supporting Information). This invariant helix stability is reminiscent of helical domains in short peptides during solvent composition titrations[38] of water into methanol (MeOH). To test for the role of the interlocking H-bond network in **F3**, we reasoned that nonpolar solvents would enhance the strengths of the H-bonds. In line with this idea, increased ratios of *n*-hexane ($\varepsilon$ = 1.9) intensified the CD signal, consistent with enhanced helical stability or helical preference. Conversely, an increased ratio of the polar protic solvent MeOH, which should compete for H-bonds, led to a decrease in the CD response; either the helix becomes less stable[39] or the impact of the amino acids on distinguishing one helix handedness over the other is much reduced. These observations indicate that the $\beta$-sheet-like H-bonds play a significant role in the folding of **F3**. This behavior is similar to that of helical peptides, which have enhanced stability in a mixture of water and trifluoroethanol,[53] where the balance between the needs of H-bonding and the hydrophobic effect is met.

**Quantifying Chloride Affinities Using UV−Vis Spectroscopic Titrations.** The chloride binding affinities (Table 1) follow the trend predicted from the foldamers' intrinsic helical stabilities, which correlates to their degree of preorganization: **F1** < **F2** < **F3**. The association constants were quantified by UV−vis titration with TBACl in 50% MeCN/THF. In this solvent mixture, **F1** and **F2** exist as random coils but **F3** is folded to some degree, and addition of chloride induces further folding. Chloride binding energies were determined using equilibrium-restricted factor analysis as implemented in Sivvu.[54] The entire wavelength range (250−500 nm) was analyzed, with the empty foldamer included as a known absorber and the 1:1 complex treated as a fitted absorbing species. No evidence for ion pairing[29d,e] or 2:1 sandwich complexes[29c−e] was found.

The *cis*-dominated isomers formed via photoisomerization by UV irradiation showed smaller binding energies than the *trans*−*trans* forms. The UV photostationary states showed the same trend in chloride affinity (**F3** > **F2** > **F1**), though with much smaller differences between the foldamers. As a result, the gap between the binding strengths for the *trans*- and *cis*-dominated states for each individual foldamer (Figure 12) becomes greater

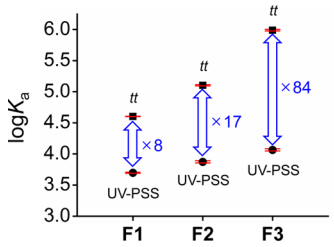


**Figure 12.** Comparison of chloride binding strengths (log $K_a$) for the *trans*−*trans* states and UV photostationary states of **F1**, **F2**, and **F3** in 50% MeCN/THF (see Table 1; error bars are shown in red, and the differentials are labeled with the $K_a^{tt}/K_a^{\text{UV-PSS}}$ values).

across the series: **F3** has an 84-fold change in chloride binding constant upon UV irradiation, while **F2** has a 17-fold change and **F1** an 8-fold change. These observations agree with the idea that the additional $\pi-\pi$ interactions (**F2**) and H-bonds (**F3**) are effective in stabilizing the chloride binding to the *trans*−*trans* photoisomers. Furthermore, we observe that the interlocking $\beta$-sheet-like H-bonds in **F3** enhance the binding differential by a factor of 5 relative to foldamer **F2**. For comparison, the extra $\pi$ overlap in **F2** produced only a 2-fold enhancement over **F1**. These findings agree with the hypothesized impact of the non-covalent interlocks in providing better stabilization of the helix in preparation for $Cl^-$ binding.

**Table 1. Chloride Binding Free Energies ($\Delta G$/kJ mol$^{-1}$), Binding Constants ($K_a$/M$^{-1}$), and Free Energy Gaps between the *trans*−*trans* Isomers and UV Photostationary States ($\Delta\Delta G$/kJ mol$^{-1}$) for F1, F2, and F3**[a]

| | *trans*−*trans* | | UV-PSS | | | |
|---|---|---|---|---|---|---|
| foldamer | $\Delta G$ | $K_a$ | $\Delta G$ | $K_a$ | $\Delta\Delta G$ | $K_a^{tt}/K_a^{\text{UV-PSS}}$ |
| **F1** | −26.27 ± 0.02 | 40300 ± 300 | −21.10 ± 0.04 | 5000 ± 80 | 5.2 ± 0.1 | 8.0 ± 0.2 |
| **F2** | −29.13 ± 0.06 | 126000 ± 3000 | −22.1 ± 0.1 | 7400 ± 300 | 7.0 ± 0.2 | 17 ± 1 |
| **F3** | −34.18 ± 0.07 | 970000 ± 30000 | −23.2 ± 0.1 | 11600 ± 500 | 11.0 ± 0.2 | 84 ± 6 |

[a]UV−vis titrations of the foldamers with TBACl in 50% MeCN/THF were performed with $\mathbf{F1}_{tt}$, **F1-UV**, $\mathbf{F2}_{tt}$, **F2-UV**, and **F3-UV** at 10 $\mu$M and $\mathbf{F3}_{tt}$ at 4 $\mu$M.


dx.doi.org/10.1021/jo501595k | J. Org. Chem. 2014, 79, 8383−8396

In the UV photostationary state, the *cis*–*trans* photoisomers that are present have residual non-covalent contacts that stabilize the folded state. On the basis of the photoisomerization studies conducted on the chloride–foldamer complexes in $CD_2Cl_2$ (Figure 9), the UV photostationary states of the foldamers have similar ratios of the isomers, with the *cis*–*trans* isomers present at ∼32%. Thus, the interactions arising when one arm is folded down onto the backbone are expected to enhance the $Cl^-$ binding energy in the UV PSS above what would be predicted for a pure *cis*–*cis* state (Figure 4). This idea was tested and verified in prior work with **F0**,[10] where the chloride affinities for the different isomers followed the order *trans*–*trans* > *cis*–*trans* > *cis*–*cis*.

**Light-Driven Binding and Release As Examined Using Electrical Conductivity.** As the photoactive foldamers **F1**, **F2**, and **F3** showed 8-, 17-, and 84-fold binding differentials, electrical conductivity measurements were utilized to confirm that these differences could be translated into light-driven binding and release of chloride. To follow the chloride concentrations, we made use of the fact that the solution conductivity ($\kappa$) of an electrolyte solution is proportional to the diffusion coefficient ($D$) and concentration ($C$) of the charged species in the solution:

$$\kappa = \frac{F}{RT}\sum_i |z_i|^2 D_i C_i$$

where $F$ is the Faraday constant, $R$ is the gas constant, $T$ is the absolute temperature, and $z_i$, $D_i$, and $C_i$ are the charge, diffusion coefficient, and concentration of species $i$, respectively. Therefore, when the chloride is bound by the receptor, the complex diffuses more slowly, which is expected to lower the solution's conductivity. This functionality was previously demonstrated with **F0**.[10] In the present experiments, a 20 $\mu$M solution of each foldamer in 50% MeCN/THF with an equimolar amount of TBACl was examined. This concentration provided the greatest contrast among the three foldamers, as predicted from the speciation curves generated using the binding data in Table 1 (see the Supporting Information for details). Upon addition of the foldamer, the conductivity dropped to a value commensurate with the strength of chloride binding. Subsequently, the solution was irradiated with UV (365 nm) and then visible (436 nm) light back and forth (Figure 13). Each foldamer showed reversible conductivity cycles, with increased conductivity for the UV PSS ($Cl^-$ release) and decreased conductivity for the visible PSS ($Cl^-$ binding).

As hypothesized, the conductivity gap between the UV and visible photostationary states increased in going from **F1** to **F3**, commensurate with the increase in the binding gap. The free chloride concentration was estimated using both the chloride binding constant obtained from UV–vis titrations and that obtained from the conductivity values. The chloride concentration could be modulated from 16 to 18 $\mu$M with **F1**, 12 to 18 $\mu$M with **F2**, and 7–17 $\mu$M with **F3**. Thus, the additional non-covalent interactions introduced along the series from **F1** to **F3** resulted in an increasing change in the chloride concentration. Furthermore, **F1** generated a larger reduction in the conductivity than the isostructural compound **F0**. This is consistent with the prediction that **F1** should have a stronger chloride binding affinity than **F0**: the electron-withdrawing ester groups on the east and west phenylenes of **F1** polarize the C–H bonds to increase the strength of CH···chloride H-bonding compared with that in **F0**, which employs electron-donating ether groups.

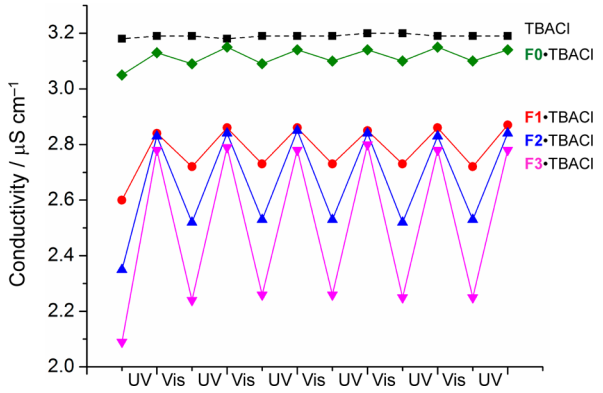


**Figure 13.** Light-driven cycles of the solution conductivity obtained upon exposure to UV (365 nm) and visible (436 nm) light. Each electrolyte solution contained equimolar concentrations (20 $\mu$M) of TBACl and foldamer **F0**, **F1**, **F2**, or **F3** in 50% MeCN/THF.

As noted above, previous studies with **F0** verified that the chloride binding affinity is strongest for the *trans*–*trans* isomer, weaker for the *cis*–*trans* isomer, and weakest for the *cis*–*cis* isomer.[10] Therefore, the initial conductivities observed in the solutions containing *trans*–*trans* foldamers present at 100% should be lower than those containing the visible photostationary states, which still retain a reasonable percentage of the *cis*–*trans* isomer (Figure 9). All of the foldamers corresponded to this trend. Moreover, the degree to which the low-conductivity state is reinstalled following irradiation with visible light (436 nm) increases across the series, with **F1**, **F2**, and **F3** showing 51%, 64%, and 77% return. This observation reflects the photostationary state ratios (Figure 9), which show that the population of the *trans*–*trans* isomer increases along the series **F1** < **F2** < **F3**. This correspondence attests to the accuracy of the proposed thermodynamic cycle that underpins the modulation in chloride affinities.

## ■ CONCLUSIONS

The light-induced shape change of azobenzene was used to switch reversibly the number of cooperative non-covalent contacts that stabilize foldamers' helices and their attendant preorganization for $Cl^-$ binding. The use of structural variants showed that $\beta$-sheet-like H-bonds that interlock the ends of the foldamer to the central helix more positively impact the differential affinity for $Cl^-$ ions. These foldamers were ultimately used to control chloride concentrations in electrolyte solutions. The predictable manner in which the helical propensities and the ensuing stabilities of the foldamers could be synthetically manipulated was paramount in enabling the improvements over the parent system. The ability to externally vary the concentrations of chloride may find use in future applications that rely upon manipulating anions, which extend from control over anion separations and the regulation of chloride availability in aqueous media[24] to modulation of anion levels during nanoparticle syntheses or in asymmetric catalysis.[6]

## ■ EXPERIMENTAL SECTION

Reagents were obtained from commercial suppliers and used as received, unless otherwise noted. 3,3′-Diiodoazobenzene[55] was prepared following a modified procedure[56] based on ones described in the literature. Column chromatography was performed on silica gel


dx.doi.org/10.1021/jo501595k | J. Org. Chem. 2014, 79, 8383–8396

(160−200 mesh), and thin-layer chromatography (TLC) was performed on precoated silica gel plates (0.25 mm thick) and observed under UV light. NMR spectra (400 and 500 MHz) were recorded at room temperature (298 K). Chemical shifts were referenced to tetramethylsilane (TMS) or residual solvent peaks. Electronic absorption (UV−vis) spectra were measured on a UV−vis−NIR spectrophotometer. Circular dichroism spectra were measured on a circular dichroism spectrometer. High-resolution electrospray ionization (ESI) mass spectrometry was performed on a trap mass spectrometer. Melting points were determined with a melting point apparatus. Conductivity measurements were done with conductivity cell (glass/platinum, $k$ = 0.1 $cm^{-1}$) and a conductivity meter.

**L-Leucine-2-(2-(2-methoxyethoxy)ethoxy)ethylamide (2).** To a solution of Boc-L-leucine (1.16 g, 5 mmol) in THF at 0 °C were added DEPBT (1.87 g, 6.26 mmol) and TEA (1.1 mL, 6.26 mmol), and the mixture was stirred for 10 min. 2-(2-(2-Methoxyethoxy)-ethoxy)ethanamine was added, and stirring was continued at rt for 24 h. The reaction mixture was extracted with ether (3 × 100 mL) and washed with brine. The organic layer was dried with $MgSO_4$, filtered, and then concentrated in vacuo. The resulting oil was purified by flash chromatography on neutral alumina with $CH_2Cl_2$/MeOH = 97:3. The light-yellowish oil product was dissolved in 20 mL of 1:1 $CH_2Cl_2$/TFA, and the solution was stirred for 2 h. The mixture was carefully neutralized with $Na_2CO_3$ solution, extracted with $CH_2Cl_2$, dried with $MgSO_4$, filtered, and evaporated to yield a clear viscous oil (733 mg, 2.65 mmol, 53% yield). $^1$H NMR ($CDCl_3$, 400 MHz): $\delta$ 7.58 (s, 1H), 3.65 (m, 6H), 3.58−3.55 (m, 4H), 3.47−3.43 (m, 2H), 3.38 (s, 3H), 3.36 (m, 1H), 1.79 (s, 2H), 1.74−1.64 (m, 2H), 1.39−1.32 (m, 1H), 0.96 (d, $J$ = 6.4 Hz, 3H), 0.93 (d, $J$ = 6.4 Hz, 3H). $^{13}$C NMR ($CDCl_3$, 100 MHz): $\delta$ 175.8, 71.9, 70.49, 70.46, 70.2, 69.9, 59.0, 53.6, 44.1, 38.8, 24.8, 23.4, 21.5. HRMS-ESI: $C_{13}H_{28}N_2O_4$ $[M{\cdot}H]^+$ calcd 277.2127, found 277.2122.

**L-Leucine-2-(2-(2-methoxyethoxy)ethoxy)ethylamide-*N*-carbonyl-3,5-diiodobenzene (3).** 3,5-Diiodobenzoic acid (1.5 g, 4.01 mmol) was refluxed with $SOCl_2$ (8 mL) for 2 h. After excess $SOCl_2$ was removed under vacuum, the resulting crude mixture of the acyl chloride compound was diluted with THF (50 mL) and cooled on an ice bath. TEA (2.2 mL, 16 mmol) and **2** (1.1 g, 4.01 mmol) were slowly added sequentially, and the mixture was stirred for 1 h with the ice bath removed. The reaction mixture was filtered, and the resulting solution was concentrated in vacuo and purified with silica gel flash column chromatography ($CH_2Cl_2$/acetone = 9:1) to yield a yellow viscous oil (2.26 g, 3.57 mmol, 89% yield). $^1$H NMR ($CDCl_3$, 400 MHz): $\delta$ 8.12 (s, 1H), 8.07 (s, 2H), 7.46 (d, $J$ = 8.4 Hz, 1H), 6.88 (s, 1H), 4.68 (m, 1H), 3.67−3.56 (m, 10H), 3.47 (m, 2H), 3.40 (s, 3H), 1.70 (m, 3H), 0.97 (d, $J$ = 5.2 Hz, 6H). $^{13}$C NMR ($CDCl_3$, 100 MHz): $\delta$ 172.6, 163.8, 147.1, 136.5, 135.3, 94.3, 71.5, 70.1, 70.0, 69.9, 69.1, 58.6, 52.3, 40.7, 39.2, 24.5, 22.7, 21.6. HRMS-ESI: $C_{20}H_{30}I_2N_2O_5$ $[M{\cdot}Na]^+$ calcd 655.0142, found 655.0124.

**L-Leucine-2-(2-(2-methoxyethoxy)ethoxy)ethylamide-*N*-carbonyl-3,5-diethynylbenzene (4).** To a degassed solution of **3** (650 mg, 1.03 mmol) and DIPA (521 mg, 5.15 mmol) in THF (40 mL) were added $Pd(PPh_3)_2Cl_2$ (14 mg, 0.021 mmol), CuI (20 mg, 0.10 mmol), and TMSA (250 mg, 2.6 mmol). The reaction mixture was stirred at rt under an argon atmosphere for 1 h and then filtered with Celite and concentrated in vacuo. The resulting crude compound was purified with flash column chromatography on silica gel with $CH_2Cl_2$/MeOH = 95:5. The brown viscous oil intermediate was dissolved in MeOH/THF (10 mL/10 mL), and $K_2CO_3$ was added. The reaction mixture was stirred at rt for 3 h, concentrated in vacuo, and flushed through a short pad of silica gel with $CH_2Cl_2$/MeOH = 95:5 to yield a yellow viscous oil (400 mg, 0.93 mmol, 89% yield). $^1$H NMR ($CDCl_3$, 400 MHz): $\delta$ 7.89 (s, 2H), 7.69 (s, 1H), 7.04 (d, $J$ = 8.0 Hz, 1H), 6.76 (s, 1H), 4.67 (m, 1H), 3.67−3.54 (m, 10H), 3.46 (m, 2H), 3.39 (s, 3H), 3.14 (s, 2H), 1.76−1.66 (m, 3H), 0.98 (s, 3H), 0.97 (s, 3H). $^{13}$C NMR ($CDCl_3$ , 100 MHz): $\delta$ 172.4, 165.4, 137.5, 134.3, 130.9, 122.5, 81.5, 78.8, 71.6, 70.2, 70.0, 69.9, 69.1, 58.6, 52.3, 41.0, 39.1, 24.6, 22.6, 21.8. HRMS-ESI: $C_{24}H_{32}N_2O_5$ $[M{\cdot}Na]^+$ calcd 451.2209, found 451.2190.

**2-(2-(2-Methoxyethoxy)ethoxy)ethyl 3,5-Diazidobenzoate (6).**[24] To a solution of 3,5-diazidobenzoic acid (2 g, 9.8 mmol) in THF (50 mL) were added DEPBT (3.5 g, 11.8 mmol), triethylene glycol monomethyl ether (2.4 g, 14.7 mmol), and TEA (1.5 g, 14.7 mmol), and the mixture was stirred at rt for 24 h. The solvent was removed under vacuum, and the residue was purified by column chromatography on silica gel with $CH_2Cl_2$/acetone = 95:5 to produce a colorless oil product. $^1$H NMR ($CDCl_3$, 400 MHz): $\delta$ 7.49 (d, $J$ = 2.0 Hz, 2H), 6.80 (s, 1H), 4.49 (t, $J$ = 4.7 Hz, 2H), 3.84 (t, $J$ = 5.1 Hz, 2H), 3.72−3.64 (m, 6H), 3.54 (m, 2H), 3.37 (s, 3H). $^{13}$C NMR ($CDCl_3$, 100 MHz): $\delta$ 164.8, 142.2, 133.2, 116.4, 113.8, 71.9, 70.69, 70.64, 70.59, 69.0, 64.7, 59.0. HRMS-ESI: $C_{14}H_{18}N_6O_5$ $[M{\cdot}H]^+$ calcd 351.1411, found 351.1419.

**F1 Azido Side Arm (7).** To a degassed solution of **5** (100 mg, 0.485 mmol), **6** (1.42 g, 3.88 mmol), and DBU (222 mg, 1.46 mmol) in toluene (60 mL) was added CuI (28 mg, 0.15 mmol). This reaction mixture was stirred at 70 °C for 2 h. The solvent was evaporated under vacuum, and the residue was purified by column chromatography on silica gel with $CH_2Cl_2$/acetone = 96:4 to produce an orange viscous oil (200 mg, 0.349 mmol, 72% yield). $^1$H NMR ($CDCl_3$, 500 MHz): $\delta$ 8.43 (s, 1H), 8.40 (s, 1H), 8.17 (s, 1H), 8.10 (d, $J$ = 7 Hz, 1H), 7.95 (m, 3H), 7.81−7.78 (m, 2H), 7.65 (t, $J$ = 7.5 Hz, 1H), 7.56−7.48 (m, 3H), 4.55 (t, $J$ = 5 Hz, 2H), 3.88 (t, $J$ = 5 Hz, 2H), 3.75−3.68 (m, 4H), 3.65 (m, 2H), 3.53 (m, 2H), 3.33 (s, 3H). $^{13}$C NMR ($CDCl_3$, 125 MHz): $\delta$ 164.2, 152.7, 152.3, 147.8, 142.3, 137.9, 133.1, 131.1, 130.6, 129.5, 128.9, 128.0, 123.3, 122.8, 119.6, 119.4, 117.9, 116.6, 114.7, 71.7, 70.52, 70.45, 70.4, 68.8, 64.8, 58.8. HRMS-ESI: $C_{28}H_{28}N_8O_5$ $[M{\cdot}H]^+$ calcd 557.2261, found 557.2255.

**Foldamer F1.** To a degassed solution of **4** (50 mg, 0.12 mmol), **7** (137 mg, 0.24 mmol), and DBU (71 mg, 0.47 mmol) in toluene (20 mL) was added CuI (7 mg, 0.04 mmol), and the mixture was stirred at 70 °C for 2 h. The solvent was evaporated in vacuo, and the residue was purified by column chromatography on silica gel with $CH_2Cl_2$/MeOH = 95:5 to yield an orange viscous oil (140 mg, 0.0908 mmol, 78% yield). $^1$H NMR (5 mM in $CD_2Cl_2$ with 10 equiv of TBACl, 500 MHz): $\delta$ 10.76 (s, 2H), 10.24 (s, 2H), 9.20 (s, 1H), 9.15 (s, 2H), 8.71 (s, 2H), 8.62 (s, 2H), 8.45 (s, 2H), 8.28 (s, 2H), 7.84 (s, 1H), 7.80 (d, $J$ = 7.3 Hz, 2H), 7.72 (d, $J$ = 7.8 Hz, 4H), 7.65 (d, $J$ = 7.8 Hz, 2H), 7.29 (m, 6H), 7.21 (t, $J$ = 7.8 Hz, 2H), 4.75 (m, 1H), 4.57 (t, $J$ = 5 Hz, 4H), 3.93 (t, $J$ = 5 Hz, 4H), 3.76 (m, 4H), 3.70 (m, 4H), 3.64 (m, 4H), 3.58 (m, 4H), 3.54−3.44 (m, 12H), three methoxy peaks (9H) overlap with a TBA peak, 1.85 (m, 3H), two methyl peaks (6H) overlap with a TBA peak. $^{13}$C NMR ($CD_2Cl_2$, 125 MHz): $\delta$ 173.2, 167.0, 165.1, 152.9, 152.7, 148.4, 148.3, 138.8, 138.4, 136.4, 133.9, 131.9, 131.8, 131.3, 129.7, 129.6, 129.4, 128.4, 128.0, 123.4, 123.2, 122.7, 121.1, 120.9, 119.1, 118.7, 114.3, 72.42, 72.39, 71.3, 71.1, 71.0, 70.8, 70.7, 70.0, 69.5, 65.5, (signals from triethylene glycol groups overlap) 59.10, 59.07, 42.2, 39.8, 25.5, 23.4, 22.3. HRMS-ESI: $C_{80}H_{88}N_{18}O_{15}$ $[M{\cdot}Cl]^-$ calcd 1575.6365, found 1575.6356.

**3,3′-Diiodoazobenzene (8).**[55,56] A solution of 3-iodoaniline (5 g, 22.8 mmol), CuBr (98 mg, 0.69 mmol), and pyridine (160 mg, 2.1 mmol) in toluene (100 mL) was stirred under open air at 60 °C for 36 h. The reaction mixture was concentrated in vacuo and purified by column chromatography on silica gel with 100% hexanes and then hexanes/ethyl acetate = 95:5 to produce an orange crystalline solid (3.01 g, 69.4 mmol, 61% yield). $^1$H NMR ($CDCl_3$, 300 MHz): $\delta$ 8.24 (s, 2H), 7.91 (d, $J$ = 7.8 Hz, 2H), 7.81 (d, $J$ = 7.8 Hz, 2H), 7.27 (t, $J$ = 7.8 Hz, 2H).

**3-Iodo-3′-(4-methoxyphenylethynyl)azobenzene (10).** To a degassed solution of 3,3′-diiodoazobenzene (**8**) (4 g, 9.22 mmol), 1-ethynyl-4-methoxybenzene (**9**) (243 mg, 1.84 mmol), and DIPA (745 mg, 7.36 mmol) in THF (80 mL) were added $PdCl_2(PPh_3)_2$ (26 mg, 0.037 mmol) and CuI (35 mg, 0.18 mmol), and the mixture was stirred under an argon atmosphere for 2 h. The resulting reaction mixture was concentrated in vacuo and purified by column chromatography on silica gel with hexanes/$CH_2Cl_2$ = 9:1 to 1:1 to generate an orange solid as the product (250 mg, 0.57 mmol, 51% yield). $^1$H NMR ($CDCl_3$, 400 MHz): $\delta$ 8.24 (s, 1H), 8.04 (s, 1H), 7.90 (d, $J$ = 7.8 Hz, 1H), 7.85 (d, $J$ = 7.8 Hz, 1H), 7.78 (d, $J$ = 7.8 Hz, 1H), 7.61 (d, $J$ = 7.4 Hz, 1H), 7.49 (d, $J$ = 8.6 Hz, 2H), 7.48 (t, $J$ = 7.8 Hz,


dx.doi.org/10.1021/jo501595k | J. Org. Chem. 2014, 79, 8383−8396

1H), 7.24 (t, $J$ = 7.8 Hz, 1H), 6.88 (d, $J$ = 8.6 Hz, 2H), 3.81 (s, 3H). $^{13}$C NMR ($CDCl_3$, 100 MHz): $\delta$ 159.8, 153.2, 152.1, 139.7, 134.0, 133.1, 130.7, 130.6, 129.1, 125.5, 124.7, 123.6, 123.0, 115.0, 114.0, 94.6, 90.4, 87.3, 55.3. HRMS-ESI: $C_{21}H_{15}IN_2O$ $[M{\cdot}H]^+$ calcd 439.0307, found 439.0318. Melting point: 116 °C.

**3-Ethynyl-3′-(4-methoxyphenylethynyl)azobenzene (11).** To a degassed solution of **10** (200 mg, 0.456 mmol) and DIPA (138 mg, 1.37 mmol) in THF (30 mL) were added $PdCl_2(PPh_3)_2$ (3 mg, 0.005 mmol), CuI (9 mg, 0.05 mmol), and TMSA (67 mg, 0.68 mmol), and the solution was stirred under Ar for 20 min. The reaction mixture was concentrated under vacuum and purified by column chromatography on silica gel with hexanes/$CH_2Cl_2$ = 9:1 to 7:3. The resulting orange solid product was dissolved in THF (5 mL) and MeOH (5 mL), to which was added 1 mL of saturated $K_2CO_3$ (in MeOH). The solution was stirred for 1 h. The solvent was evaporated, and the residue was filtered through a short pad of silica gel with $CH_2Cl_2$, yielding an orange solid product (130 mg, 0.386 mmol, 85% yield). $^1$H NMR ($CDCl_3$, 400 MHz): $\delta$ 8.06 (s, 2H), 7.91 (d, $J$ = 7.8 Hz, 1H), 7.87 (d, $J$ = 7.8 Hz, 1H), 7.61 (d, $J$ = 7.8 Hz, 1H), 7.60 (d, $J$ = 7.4 Hz, 1H), 7.49 (m, 4H), 6.89 (d, $J$ = 8.6 Hz, 2H), 3.82 (s, 3H), 3.14 (s, 1H). $^{13}$C NMR ($CDCl_3$, 100 MHz): $\delta$ 159.8, 152.3, 152.2, 134.5, 133.9, 133.2, 129.12, 129.10, 126.4, 125.5, 124.7, 123.6, 123.2, 122.9, 115.0, 114.0, 90.3, 87.3, 82.8, 78.0, 55.3. HRMS-ESI: $C_{23}H_{16}N_2O$ $[M{\cdot}H]^+$ calcd 337.1341, found 337.1335. Melting point: 113 °C.

**F2 Azido Side Arm (12).** To a degassed solution of **11** (180 mg, 0.535 mmol), **6** (1.8 g, 5.14 mmol), and DBU (244 mg, 1.61 mmol) in toluene was added CuI (31 mg, 0.16 mmol), and the solution was stirred at 70 °C for 30 min under argon. The reaction mixture was concentrated in vacuo and purified by column chromatography on silica gel with $CH_2Cl_2$/acetone = 95:5, producing an orange viscous oil (255 mg, 0.371 mmol, 69% yield). $^1$H NMR ($CDCl_3$, 400 MHz): $\delta$ 8.45 (s, 1H), 8.43 (s, 1H), 8.19 (s, 1H), 8.14 (d, $J$ = 7.8 Hz, 1H), 8.12 (s, 1H), 7.98 (d, $J$ = 7.8 Hz, 1H), 7.93 (d, $J$ = 8.2 Hz, 1H), 7.83 (s, 1H), 7.81 (s, 1H), 7.67 (t, $J$ = 7.8 Hz, 1H), 7.64 (d, $J$ = 7.8 Hz, 1H), 7.52 (m, 3H), 6.91 (d, $J$ = 8.6 Hz, 2H), 4.57 (t, $J$ = 5.0 Hz, 2H), 3.89 (t, $J$ = 5.0 Hz, 2H), 3.85 (s, 3H), 3.75−3.65 (m, 4H), 3.66 (m, 2H), 3.53 (t, $J$ = 5.0 Hz, 2H), 3.34 (s, 3H). $^{13}$C NMR ($CDCl_3$, 100 MHz): $\delta$ 164.4, 169.7, 152.7, 152.2, 147.9, 142.5, 138.0, 133.7, 133.2, 133.1, 131.8, 129.7, 129.0, 128.3, 125.4, 124.6, 123.6, 122.7, 119.7, 119.6, 117.9, 116.7, 114.92, 114.86, 114.0, 90.2, 87.3, 71.8, 70.61, 70.55, 70.5, 68.9, 64.9, 58.9, 55.2. HRMS-ESI: $C_{37}H_{34}N_8O_6$ $[M{\cdot}H]^+$ calcd 687.2680, found 687.2682.

**Foldamer F2.** To a degassed solution of **4** (50 mg, 0.12 mmol), **12** (164 mg, 0.24 mmol), and DBU (71 mg, 0.47 mmol) was added CuI (7 mg, 0.04 mmol), and the solution was stirred at 70 °C for 30 min. The reaction mixture was concentrated in vacuo and purified by column chromatography on silica gel with $CH_2Cl_2$/MeOH = 95:5 to produce an orange viscous oil (167 mg, 0.093 mmol, 79% yield). $^1$H NMR (5 mM in $CD_2Cl_2$ with 10 equiv of TBACl, 500 MHz): $\delta$ 10.86 (s, 2H), 10.34 (s, 2H), 9.29 (s, 1H), 9.13 (s, 2H), 8.70 (s, 2H), 8.54 (s, 2H), 8.38 (s, 2H), 8.29 (s, 2H), 7.82 (s, 2H), 7.75 (d, $J$ = 7.3 Hz, 2H), 7.68 (d, $J$ = 8.8 Hz, 2H), 7.66 (d, $J$ = 8.8 Hz, 2H), 7.57 (br, 1H), 7.40 (t, $J$ = 6.6 Hz, 1H), 7.35 (t, $J$ = 7.7 Hz, 2H), 7.33 (d, $J$ = 8.8 Hz, 4H), 7.25 (t, $J$ = 7.7 Hz, 2H), 7.22 (t, $J$ = 7.7 Hz, 2H), 6.83 (d, $J$ = 8.8 Hz, 4H), 4.76 (m, 1H), 4.57 (t, $J$ = 4.8 Hz, 4H), 3.91 (t, $J$ = 4.8 Hz, 4H), 3.82 (s, 6H), 3.74 (m, 4H), 3.68 (m, 4H), 3.60 (m, 8H), 3.56 (m, 4H), 3.51−3.46 (m, 8H), 3.33 (s, 3H), a methoxy peak (3H) overlaps with a TBA peak, 1.85 (m, 3H), two methyl groups overlap with a TBA peak. $^{13}$C NMR ($CD_2Cl_2$, 125 MHz): $\delta$ 173.0, 167.1, 165.1, 160.4, 152.7, 152.4, 148.4, 148.2, 138.6, 138.5, 136.4, 133.8, 133.7, 133.5, 132.1, 131.8, 129.6, 129.4, 128.5, 128.3, 126.3, 124.9, 123.4, 122.9, 122.8, 122.5, 121.2, 120.7, 119.0, 118.8, 115.3, 114.5, 114.2, 90.7, 87.7, 72.4, 71.3, 71.03, 70.98, 70.84, 70.76, 70.1, 69.5, 59.1, (some Tg signals overlap) 55.9, 42.2, 39.8, 30.2, 25.6, 23.4, 22.4. HRMS-ESI: $C_{98}H_{100}N_{18}O_{17}$ $[M{\cdot}Cl]^-$ calcd 1835.7202, found 1835.7235.

**L-Leucine-*n*-hexylamide (14).** To a solution of Boc-L-leucine (2 g, 8.65 mmol), DEPBT (2.85 g, 9.52 mmol), and TEA (1.14 g, 11.3 mmol) in THF (50 mL) was added *n*-hexylamine (1.14 g, 11.3 mmol), and the mixture was stirred overnight. The reaction mixture was extracted with ether (×3) and washed with water. The organic phase was dried with $MgSO_4$, filtered, and concentrated in vacuo. The crude mixture was purified by column chromatography on neutral alumina with $CH_2Cl_2$/MeOH = 98:2. The resulting colorless waxy solid was dissolved in $CH_2Cl_2$ (20 mL), to which was added trifluoroacetic acid (6 mL). The reaction mixture was stirred for 3 h, neutralized with concentrated $Na_2CO_3$ solution, extracted with $CH_2Cl_2$ (×5), dried with $MgSO_4$, filtered, and concentrated in vacuo to yield a yellow viscous oil product (1.56 g, 7.28 mmol, 84% yield). $^1$H NMR ($CDCl_3$, 400 MHz): $\delta$ 7.33 (s, 1H), 3.38 (br, 1H), 3.23 (m, 2H), 1.72 (m, 3H), 1.50 (m, 4H), 1.30 (m, 6H), 0.95 (m, 6H), 0.89 (m, 3H). $^{13}$C NMR ($CDCl_3$, 100 MHz): $\delta$ 175.3, 53.4, 44.1, 38.9, 31.3, 29.5, 26.5, 24.7, 23.3, 22.4, 21.2, 13.8. HRMS-ESI: $C_{12}H_{26}N_2O$ $[M{\cdot}H]^+$ calcd 215.2123, found 215.2124.

**L-Leucine-*n*-hexylamide-*N*-carbonyl-4-iodobenzene (15).** *p*-Iodobenzoic acid (1.34 g, 5.39 mmol) was dissolved in $SOCl_2$ (10 mL), and the solution was refluxed for 1 h. Excess $SOCl_2$ was removed in vacuo, and the resulting solid was dissolved in $CH_2Cl_2$ (30 mL) and TEA (3 mL). **14** (1.1 g, 5.1 mmol) was added dropwise under ice-bath conditions, and the resulting solution was warmed to rt and then stirred for 1 h. The reaction mixture was extracted with $CH_2Cl_2$ and washed with 3 M HCl aqueous solution. The organic phase was dried with $MgSO_4$, filtered, and concentrated in vacuo to produce a white solid (2.3 g, 5.1 mmol, quantitative yield). $^1$H NMR ($CDCl_3$, 400 MHz): $\delta$ 7.73 (d, $J$ = 8.0 Hz, 2H), 7.49 (d, $J$ = 8.0 Hz, 2H), 7.15 (d, $J$ = 7.8 Hz, 1H), 6.59 (s, 1H), 4.67 (m, 1H), 3.26−3.10 (m, 2H), 1.73 (m, 3H), 1.46 (m, 2H), 1.26 (s, 6H), 0.96 (s, 6H), 0.86 (m, 3H). $^{13}$C NMR ($CDCl_3$, 100 MHz): $\delta$ 172.0, 166.6, 137.6, 133.2, 128.8, 98.7, 52.4, 41.3, 39.6, 31.4, 29.3, 26.5, 24.9, 22.8, 22.5, 22.4, 14.0. HRMS-ESI: $C_{19}H_{29}IN_2O_2$ $[M{\cdot}Na]^+$ calcd 467.1172, found 467.1190. Melting point: 134 °C.

**L-Leucine-*n*-hexylamide-*N*-carbonyl-4-ethynylbenzene (16).** To a degassed solution of **15** (1.5 g, 3.38 mmol) and DIPA (182 mg, 1.8 mmol) in THF (50 mL) were added $PdCl_2(PPh_3)_2$ (48 mg, 0.068 mmol), CuI (64 mg, 0.34 mmol), and TMSA (432 mg, 4.39 mmol), and the solution was stirred under argon for 1 h. The reaction mixture was filtered through a pad of Celite and concentrated in vacuo. The resulting crude mixture was purified by column chromatography on silica gel with $CH_2Cl_2$/MeOH = 95:5. The resulting brownish oil product was dissolved in THF (30 mL) and MeOH (30 mL), to which was added 5 mL of saturated $K_2CO_3$ (in MeOH). The mixture was stirred for 2 h, concentrated in vacuo, and filtered through a short pad of silica gel with $CH_2Cl_2$/MeOH = 95:5 solution to provide a slightly brown solid (1.08 g, 3.15 mmol, 93% yield). $^1$H NMR ($CDCl_3$, 400 MHz): $\delta$ 7.75 (d, $J$ = 8.2 Hz, 2H), 7.51 (d, $J$ = 8.2 Hz, 2H), 7.07 (d, $J$ = 7.8 Hz, 1H), 6.55 (s, 1H), 4.69 (m, 1H), 3.31−3.12 (m, 2H), 3.20 (s, 1H), 1.74 (m, 3H), 1.48 (m, 2H), 1.26 (s, 6H), 0.98 (m, 6H), 0.86 (m, 3H). $^{13}$C NMR ($CDCl_3$, 100 MHz): $\delta$ 172.5, 168.6, 133.7, 131.9, 127.2, 125.3, 82.7, 79.4, 52.6, 41.2, 39.5, 21.4, 29.3, 26.5, 24.9, 22.8, 22.5, 22.3, 13.9. HRMS-ESI: $C_{21}H_{30}N_2O_2$ $[M{\cdot}Na]^+$ calcd 365.2205, found 365.2216. Melting point: 107 °C.

**3-(4-(L-Leucine-*n*-hexylamide-*N*-carbonyl)phenylethynyl)-3′-iodoazobenzene (17).** To a degassed solution of **16** (631 mg, 1.84 mmol), 3,3′-diiodoazobenzene (4 g, 9.22 mmol), and DIPA (745 mg, 7.36 mmol) in THF (100 mL) were added $PdCl_2(PPh_3)_2$ (26 mg, 0.037 mmol) and CuI (35 mg, 0.18 mmol), and the solution was stirred under argon for 1 h. The reaction mixture was concentrated in vacuo and purified by column chromatography on silica gel with $CH_2Cl_2$/acetone = 95:5 to provide an orange waxy solid product (790 mg, 1.22 mmol, 66% yield). $^1$H NMR ($CDCl_3$, 500 MHz): $\delta$ 8.25 (s, 1H), 8.07 (s, 1H), 7.90 (d, $J$ = 7.8 Hz, 1H), 7.89 (d, $J$ = 7.8 Hz, 1H), 7.80 (d, $J$ = 7.8 Hz, 1H), 7.77 (d, $J$ = 8.3 Hz, 2H), 7.63 (d, $J$ = 7.8 Hz, 1H), 7.60 (d, $J$ = 8.3 Hz, 2H), 7.50 (t, $J$ = 8.3 Hz, 1H), 7.26 (t, $J$ = 8.3 Hz, 1H), 6.76 (d, $J$ = 8.3 Hz, 1H), 6.20 (t, $J$ = 4.9 Hz, 1H), 4.64 (m, 1H), 3.27 (m, 2H), 1.83−1.69 (m, 3H), 1.52 (m, 2H), 1.30 (m, 6H), 1.01 (s, 3H), 1.00 (s, 3H), 0.89 (t, $J$ = 6.8 Hz, 3H). $^{13}$C NMR ($CDCl_3$, 125 MHz): $\delta$ 171.8, 166.6, 153.4, 152.3, 139.9, 134.2, 133.6, 131.8, 130.9, 130.6, 129.3, 127.2, 126.6, 125.9, 124.0, 123.7, 123.5, 94.5, 91.0, 89.4, 52.4, 41.6, 39.7, 31.4, 29.5, 26.5, 25.1, 22.9, 22.50, 22.48, 13.9 (a single peak is missing, presumably because of overlap in the aromatic


dx.doi.org/10.1021/jo501595k | J. Org. Chem. 2014, 79, 8383−8396

region). HRMS-ESI: $C_{33}H_{37}IN_4O_2$ $[M{\cdot}H]^+$ calcd 649.2040, found 649.2023. Melting point: 215 °C.

**3-Ethynyl-3′-(4-(L-leucine-*n*-hexylamide-*N*-carbonyl)-phenylethynyl)azobenzene (18).** To a degassed solution of **17** (260 mg, 0.4 mmol) and TEA (81 mg, 0.8 mmol) in THF (10 mL) were added $PdCl_2(PPh_3)_2$ (3 mg, 0.004 mmol), CuI (8 mg, 0.04 mmol), and TMSA (59 mg, 0.6 mmol) and the solution was stirred under argon for 30 min. The reaction mixture was directly loaded onto a silica gel column and purified with $CH_2Cl_2$/acetone = 96:4. The resulting orange waxy solid was dissolved in THF (5 mL), MeOH (5 mL), and 1 mL of saturated $K_2CO_3$ (in MeOH). The reaction mixture was stirred for 1 h, concentrated in vacuo, and filtered through a short pad of silica gel with $CH_2Cl_2$/MeOH = 95:5 to provide an orange solid (181 mg, 0.33 mmol, 83%). $^1$H NMR ($CDCl_3$, 400 MHz): $\delta$ 8.08 (s, 1H), 8.04 (s, 1H), 7.91 (m, 2H), 7.79 (d, $J$ = 8.2 Hz, 2H), 7.64 (d, $J$ = 7.4 Hz, 1H), 7.61 (d, $J$ = 7.4 Hz, 1H), 7.59 (d, $J$ = 8.2 Hz, 2H), 7.50 (t, $J$ = 7.8 Hz, 1H), 7.49 (t, $J$ = 7.8 Hz, 1H), 7.09 (d, $J$ = 8.6 Hz, 1H), 6.60 (t, $J$ = 5.9 Hz, 1H), 4.72 (m, 1H), 3.33−3.14 (m, 2H), 3.16 (s, 1H), 1.77 (m, 3H), 1.50 (m, 2H), 1.27 (m, 6H), 1.00 (m, 6H), 0.87 (m, 3H). $^{13}$C NMR ($CDCl_3$, 100 MHz): $\delta$ 172.1, 166.7, 152.2, 152.1, 134.5, 134.1, 133.4, 131.7, 129.2, 129.1, 127.3, 126.4, 125.7, 123.8, 123.6, 123.6, 123.1, 90.9, 89.3, 82.8, 78.1, 52.4, 41.4, 39.6, 31.4, 29.4, 26.5, 25.0, 22.9, 22.5, 22.4, 14.0. HRMS-ESI: $C_{35}H_{38}N_4O_2$ $[M{\cdot}Na]^+$ calcd 569.2892, found 569.2885. Melting point: 173 °C.

**F3 Azido Side Arm (19).** To a degassed solution of **18** (160 mg, 0.293 mmol), **6** (3 g, 8.56 mmol), and DBU (180 mg, 1.17 mmol) in toluene (100 mL) was added CuI (17 mg, 0.088 mmol), and the mixture was stirred at 70 °C for 1 h. The reaction mixture was concentrated in vacuo and purified by column chromatography on silica gel with $CH_2Cl_2$/acetone = 95:5 and then with $CH_2Cl_2$/MeOH = 97:3 to yield an orange viscous oil (205 mg, 0.23 mmol, 78% yield). $^1$H NMR ($CDCl_3$, 400 MHz): $\delta$ 8.42 (s, 1H), 8.37 (s, 1H), 8.15 (s, 1H), 8.10 (s, 1H), 8.08 (d, $J$ = 7.8 Hz, 1H), 7.93 (s, 1H), 7.91 (s, 1H), 7.77 (m, 4H), 7.63 (m, 2H), 7.57 (d, $J$ = 8.6 Hz, 2H), 7.49 (t, $J$ = 7.8 Hz, 1H), 7.11 (d, $J$ = 8.2 Hz, 1H), 6.64 (t, $J$ = 5.8 Hz, 1H), 4.72 (m, 1H), 4.55 (t, $J$ = 4.7 Hz, 2H), 3.87 (t, $J$ = 4.7 Hz, 2H), 3.75−3.63 (m, 6H), 3.52 (m, 2H), 3.33 (s, 3H), 3.35−3.16 (m, 2H), 1.81−1.72 (m, 3H), 1.50 (m, 2H), 1.27 (m, 6H), 1.00 (m, 6H), 0.87 (m, 3H). $^{13}$C NMR ($CDCl_3$, 100 MHz): $\delta$ 172.2, 166.6, 164.2, 152.4, 151.9, 147.7, 142.7, 142.3, 137.8, 133.8, 133.3, 133.1, 131.4, 130.6, 129.5, 129.0, 128.2, 127.2, 126.1, 125.5, 123.6, 123.40, 123.35, 119.5, 119.4, 117.9, 116.5, 114.6, 90.8, 89.2, 71.7, 70.5, 70.40, 70.36, 64.8, 58.7, 52.4, 41.2, 39.5, 31.3, 29.2, 26.4, 24.8, 22.7, 22.4, 22.3, 13.8. HRMS-ESI: $C_{49}H_{56}N_{10}O_7$ $[M{\cdot}Na]^+$ calcd 919.4231, found 919.4269.

**Foldamer F3.** To a degassed solution of **4** (36 mg, 0.085 mmol), **19** (160 mg, 0.18 mmol), and DBU (39 mg, 0.25 mmol) in toluene (10 mL) was added CuI (5 mg, 0.03 mmol), and the solution was stirred at 70 °C for 1 h. The mixture was concentrated in vacuo and purified by column chromatography on silica gel with $CH_2Cl_2$/MeOH = 95:5 and then 93:7 to provide an orange viscous oil. Further extraction with $CH_2Cl_2$ and deionized water gave a pure compound suitable for conductivity experiments (111 mg, 0.05 mmol, 59% yield). $^1$H NMR (5 mM in $CD_2Cl_2$ with 10 equiv of TBACl, 500 MHz): $\delta$ 10.97 (s, 2H), 10.41 (s, 2H), 9.44 (s, 1H), 9.04 (s, 2H), 8.83 (d, $J$ = 8.8 Hz, 1H), 8.65 (s, 2H), 8.35 (s, 2H), 8.31 (s, 2H), 8.29 (t, $J$ = 5.9 Hz, 1H), 8.20 (s, 2H), 7.94 (d, $J$ = 8.3 Hz, 2H), 7.85 (s, 2H), 7.70 (d, $J$ = 8.3 Hz, 4H), 7.73−7.68 (m, 6H), 7.34 (d, $J$ = 7.3 Hz, 2H), 7.32 (d, $J$ = 7.8 Hz, 2H), 7.28 (d, $J$ = 7.3 Hz, 2H), 7.21 (d, $J$ = 8.3 Hz, 4H), 5.07 (m, 1H), 5.03 (m, 2H), 4.61 (t, $J$ = 5.4 Hz, 4H), 3.97 (t, $J$ = 4.9 Hz, 4H), 3.81 (m, 4H), 3.73 (m, 4H), 3.64 (m, 10H), 3.58 (m, 4H), 3.52 (m, 4H), 3.48 (m, 2H), 3.32 (s, 9H), 3.26−3.14 (m, 4H, partially overlaps with a TBA peak), 2.04 (m, 2H), 1.89 (m, 4H), 1.75 (m, 3H), 1.54 (m, 4H), 1.28 (m, 12H), six methyl peaks (18H) overlap with a TBA peak, 0.84 (m, 6H). $^{13}$C NMR (6 mM $CD_2Cl_2$ with 8 equiv of TBACl, 125 MHz): $\delta$ 172.97, 172.94, 169.6, 167.5, 165.2, 152.6, 152.0, 148.5, 148.3, 138.6, 138.3, 137.7, 134.4, 133.6, 133.5, 132.1, 132.0, 131.9, 131.8, 130.7, 129.8, 129.5, 128.4, 127.7, 125.9, 125.7, 124.2, 123.5, 122.9, 121.6, 119.7, 119.4, 118.3, 114.7, 90.6, 90.2, 72.5, 71.4, 71.2, 71.1, 71.04, 71.02, 70.99, 70.01, 69.7, 65.4, 59.2, 53.2, 52.5, 41.7, 41.3, 40.1, 32.1, 30.2, 30.0, 27.2, 25.9, 25.7, 23.6, 23.4, 23.2, 23.1, 14.4. HRMS-ESI: $C_{122}H_{144}N_{22}O_{19}$ $[M{\cdot}Cl]^-$ calcd 2256.0667, found 2256.0601.

**Oligomer 20.** To a degassed solution of **4** (40 mg, 0.093 mmol), 1-azido-4-(*tert*-butyl)benzene (36 mg, 0.21 mmol), and tris[(1-benzyl-1*H*-1,2,3-triazol-4-yl)methyl]amine (TBTA) (5 mg, 0.009 mmol) in THF (3 mL), EtOH (3 mL), and water (2 mL) were added $CuSO_4{\cdot}5H_2O$ (2 mg, 0.009 mmol) and sodium ascorbate (4 mg, 0.019 mmol). The reaction mixture was stirred for 2 h, extracted with $CH_2Cl_2$, dried with $MgSO_4$, concentrated in vacuo, and then purified by column chromatography on silica gel with $CH_2Cl_2$/MeOH = 98:2 to provide a white solid product (65 mg, 0.083 mmol, 89% yield). $^1$H NMR ($CD_2Cl_2$, 400 MHz): $\delta$ 8.57 (s, 1H), 8.42 (s, 2H), 8.25 (s, 2H), 7.74 (d, $J$ = 8.6 Hz, 4H), 7.61 (s, 1H), 7.59 (d, $J$ = 8.6 Hz, 4H), 6.94 (t, $J$ = 5.3 Hz, 1H), 4.74 (m, 1H), 3.59−3.43 (m, 12H), 3.32 (s, 3H), 1.79 (m, 3H), 1.38 (s, 18H), 1.00 (m, 6H). $^{13}$C NMR ($CDCl_3$, 125 MHz): $\delta$ 172.7, 166.9, 152.0, 146.8, 135.0, 134.3, 131.1, 126.5, 125.4, 124.1, 119.9, 118.5, 71.8, 70.4, 70.3, 70.1, 69.5, 58.8, 52.6, 41.2, 39.3, 34.6, 31.1, 24.8, 23.0, 21.8. HRMS-ESI: $C_{44}H_{58}N_8O_5$ $[M{\cdot}Na]^+$ calcd 801.4428, found 801.4406. Melting point: 115 °C.

## ■ ASSOCIATED CONTENT

### Ⓢ Supporting Information

$^1$H and $^{13}$C NMR spectra, 2D COSY and NOESY NMR spectra, UV−vis absorption spectra of photostationary states, circular dichroism and UV−vis titration spectra, Sivvu analysis, and conductivity measurements. This material is available free of charge via the Internet at http://pubs.acs.org.

## ■ AUTHOR INFORMATION

### Corresponding Author

*E-mail: aflood@indiana.edu.

### Notes

The authors declare no competing financial interest.

## ■ ACKNOWLEDGMENTS

This work was supported by the Chemical Sciences, Geosciences, and Biosciences Division, Office of Basic Energy Sciences, Office of Science, U.S. Department of Energy.

## ■ REFERENCES

(1) Nelson, D. L.; Lehninger, A. L.; Cox, M. M. *Lehninger Principles of Biochemistry*, 5th ed.; W. H. Freeman: New York, 2008.

(2) (a) *Supramolecular Chemistry of Anions*; Bianchi, A., Bowman-James, K., García-España, E., Eds.; Wiley-VCH: New York, 1997. (b) Sessler, J. L.; Gale, P. A.; Cho, W.-S. *Anion Receptor Chemistry*; RSC Publishing: Cambridge, U.K., 2006.

(3) Wright, E. M.; Diamond, J. M. *Physiol. Rev.* **1977**, *57*, 109−156.

(4) (a) Dutzler, R.; Campbell, E. B.; Cadene, M.; Chait, B. T.; MacKinnon, R. *Nature* **2002**, *415*, 287−294. (b) Dutzler, R.; Campbell, E. B.; MacKinnon, R. *Science* **2003**, *300*, 108−112. (c) Novarino, G.; Weinert, S.; Rickheit, G.; Jentsch, T. J. *Science* **2010**, *328*, 1398−1401.

(5) Ooi, T.; Maruoka, K. *Angew. Chem., Int. Ed.* **2007**, *46*, 4222−4266.

(6) Rauniyar, V.; Lackner, A. D.; Hamilton, G. L.; Toste, F. D. *Science* **2011**, *334*, 1681−1684.

(7) Moyer, B. A.; Bonnesen, P. V.; Custelcean, R.; Delmau, L. H.; Hay, B. P. *Kem. Ind.* **2005**, *54*, 65−87.

(8) Wilson, A. M.; Bailey, P. J.; Tasker, P. A.; Turkington, J. R.; Grant, R. A.; Love, J. B. *Chem. Soc. Rev.* **2014**, *43*, 123−134.

(9) Moyer, B. A.; Custelcean, R.; Hay, B. P.; Sessler, J. L.; Bowman-James, K.; Day, V. W.; Kang, S.-O. *Inorg. Chem.* **2013**, *52*, 3473−3490.

(10) Hua, Y.; Flood, A. H. *J. Am. Chem. Soc.* **2010**, *132*, 12838−12840.

(11) Fortin, D. L.; Banghart, M. R.; Dunn, T. W.; Borgse, K.; Wagenaar, D. A.; Gaudry, Q.; Karakossian, M. H.; Otis, T. S.; Kristan, W. B.; Trauner, D.; Kramer, R. H. *Nat. Methods* **2008**, *5*, 331−338.

(12) Beharry, A. A.; Woolley, G. A. *Chem. Soc. Rev.* **2011**, *40*, 4422−4437.
(13) Sather, A. C.; Berryman, O. B.; Rebek, J., Jr. *Chem. Sci.* **2013**, *4*, 3601−3605.
(14) (a) Shinkai, S.; Ogawa, T.; Nakaji, T.; Kusano, Y.; Nanabe, O. *Tetrahedron Lett.* **1979**, *20*, 4569−4572. (b) Shinkai, S. In *Molecular Switches*; Feringa, B. L., Ed.; Wiley-VCH: Weinheim, Germany, 2001; pp 281−307.
(15) Shinkai, S.; Nakaji, T.; Ogawa, T.; Shigematsu, K.; Manabe, O. *J. Am. Chem. Soc.* **1981**, *103*, 111−115.
(16) Schobert, B.; Lanyi, J. K. *J. Biol. Chem.* **1982**, *257*, 306−313.
(17) (a) Oesterhelt, D.; Kolbe, M.; Besir, H.; Essen, L. O. *Science* **2000**, *288*, 1390−1396. (b) Essen, L. O. *Curr. Opin. Struct. Biol.* **2002**, *12*, 516−522.
(18) Lee, S.; Flood, A. H. *J. Phys. Org. Chem.* **2013**, *26*, 79−86.
(19) Bencini, A.; Bianchi, A.; Giorgi, C.; Romagnoli, E.; Lodeiro, C.; Saint-Maurice, A.; Pina, F.; Valtancoli, B. *Supramol. Chem.* **2001**, *13*, 277−285.
(20) Shimasaki, T.; Kato, S.-i.; Ideta, K.; Goto, K.; Shinmyozu, T. *J. Org. Chem.* **2007**, *72*, 1073−1087.
(21) Wang, Y.; Bie, F.; Jiang, H. *Org. Lett.* **2010**, *12*, 3630−3633.
(22) Li, Z.; Zhang, C.; Ren, Y.; Yin, J.; Liu, S. H. *Org. Lett.* **2011**, *13*, 6022−6025.
(23) Han, M.; Michel, R.; He, B.; Chen, Y.-S.; Stalke, D.; John, M.; Clever, G. H. *Angew. Chem., Int. Ed.* **2013**, *52*, 1319−1323.
(24) Hua, Y.; Liu, Y.; Chen, C.-H.; Flood, A. H. *J. Am. Chem. Soc.* **2013**, *135*, 14401−14412.
(25) *Foldamers: Structure, Properties and Applications*; Hecht, S., Huc, I., Eds.; Wiley-VCH: Weinheim, Germany, 2007.
(26) (a) Prince, R. B.; Okada, T.; Moore, J. S. *Angew. Chem., Int. Ed.* **1999**, *38*, 233−236. (b) Hou, J. L.; Jia, M. X.; Jiang, X. K.; Li, Z. T.; Chen, G. J. *J. Org. Chem.* **2004**, *69*, 6228−6237. (c) Inouye, M.; Waki, M.; Abe, H. *J. Am. Chem. Soc.* **2004**, *126*, 2022−2027. (d) Abe, H.; Masuda, N.; Waki, M.; Inouye, M. *J. Am. Chem. Soc.* **2005**, *127*, 16189−16196. (e) Garric, J.; Leger, J. M.; Huc, I. *Angew. Chem., Int. Ed.* **2005**, *44*, 1954−1958. (f) Suk, J. M.; Jeong, K. S. *J. Am. Chem. Soc.* **2008**, *130*, 11868−11869. (g) Haketa, Y.; Maeda, H. *Chem.—Eur. J.* **2011**, *17*, 1485−1492.
(27) Juwarker, H.; Jeong, K. S. *Chem. Soc. Rev.* **2010**, *39*, 3664−3674.
(28) Nelson, J. C.; Saven, J. G.; Moore, J. S.; Wolynes, P. G. *Science* **1997**, *277*, 1793−1796.
(29) (a) Li, Y.; Flood, A. H. *Angew. Chem., Int. Ed.* **2008**, *47*, 2649−2652. (b) Li, Y.; Flood, A. H. *J. Am. Chem. Soc.* **2008**, *130*, 12111−12122. (c) Li, Y.; Pink, M.; Karty, J. A.; Flood, A. H. *J. Am. Chem. Soc.* **2008**, *130*, 17293−17295. (d) Hua, Y.; Ramabhadran, R. O.; Karty, J. A.; Raghavachari, K.; Flood, A. H. *Chem. Commun.* **2011**, *47*, 5979−5981. (e) Ramabhadran, R. O.; Liu, Y.; Hua, Y.; Ciardi, M.; Flood, A. H.; Raghavachari, K. *J. Am. Chem. Soc.* **2014**, *136*, 5078−5089.
(30) Triazole CH···anion interactions from 2008 to 2009: (a) Juwarker, H.; Lenhardt, J. M.; Pham, D. M.; Craig, S. L. *Angew. Chem., Int. Ed.* **2008**, *47*, 3740−3743. (b) Hecht, S.; Meudtner, R. M. *Angew. Chem., Int. Ed.* **2008**, *47*, 4926−4930. (c) Kumar, A.; Pandey, P. S. *Org. Lett.* **2008**, *10*, 165−168. (d) Wang, Y.; Li, F.; Han, Y.; Wang, F.; Jiang, H. *Chem.—Eur. J.* **2009**, *15*, 9424−9433. (e) Fisher, M. G.; Gale, P. A.; Hiscock, J. R.; Hursthouse, M. B.; Light, M. E.; Schmidtchen, F. P.; Tong, C. C. *Chem. Commun.* **2009**, 3017−3019. (f) Juwarker, H.; Lenhardt, J. M.; Castillo, J. C.; Zhao, E.; Krishnamurthy, S.; Jamiolkowski, R. M.; Kim, K. H.; Craig, S. L. *J. Org. Chem.* **2009**, *74*, 8924−8934. (g) Mullen, K. M.; Mercurio, J.; Serpell, C. J.; Beer, P. D. *Angew. Chem., Int. Ed.* **2009**, *48*, 4781−4784. (h) Romero, T.; Caballero, A.; Tarraga, A.; Molina, P. *Org. Lett.* **2009**, *11*, 3466−3469. (i) Wang, Y.; Li, F.; Han, Y.; Wang, F.; Jiang, H. *Chem.—Eur. J.* **2009**, *15*, 9424−9433.
(31) Triazole CH···anion interactions from 2010 to 2012: (a) Yano, M.; Tong, C. C.; Light, M. E.; Schmidtchen, F. P.; Gale, P. A. *Org. Biomol. Chem.* **2010**, *8*, 4356−4363. (b) Kim, J. S.; Park, S. Y.; Kim, S. H.; Thuery, P.; Souane, R.; Matthews, S. E.; Vicens, J. *Bull. Korean Chem. Soc.* **2010**, *31*, 624−629. (c) Schulze, B.; Friebe, C.; Hager, M. D.; Gunther, W.; Kohn, U.; Jahn, B. O.; Gorls, H.; Schubert, U. S. *Org. Lett.* **2010**, *12*, 2710−2713. (d) Sessler, J. L.; Cai, J.; Gong, H.-Y.; Yang, X.; Arambula, J. F.; Hay, B. P. *J. Am. Chem. Soc.* **2010**, *132*, 14058−14060. (e) Zhao, Y.; Li, Y.; Li, Y.; Huang, C.; Liu, H.; Lai, S.-W.; Che, C.-M.; Zhu, D. *Org. Biomol. Chem.* **2010**, *8*, 3923−3927. (f) Cao, Q.-Y.; Pradhan, T.; Kim, S.; Kim, J. S. *Org. Lett.* **2011**, *13*, 4386−4389. (g) Chhatra, R. K.; Kumar, A.; Pandey, P. S. *J. Org. Chem.* **2011**, *76*, 9086−9089. (h) Garcia, F.; Torres, M. R.; Matesanz, E.; Sanchez, L. *Chem. Commun.* **2011**, *47*, 5016−5018. (i) Haridas, V. H.; Sahu, S.; Venugopalan, P. *Tetrahedron* **2011**, *67*, 727−733. (j) Lee, C.-H.; Lee, S.; Yoon, H.; Jang, W.-D. *Chem.—Eur. J.* **2011**, *17*, 13898−13903. (k) Ohmatsu, K.; Kiyokawa, M.; Ooi, T. *J. Am. Chem. Soc.* **2011**, *133*, 1307−1309. (l) Wang, Y.; Xiang, J. F.; Jiang, H. *Chem.—Eur. J.* **2011**, *17*, 613−619. (m) Yamato, T.; Ni, X. L.; Zeng, X.; Redshaw, C. *J. Org. Chem.* **2011**, *76*, 5696−5702. (n) Li, Y.-J.; Xu, L.; Yang, W.-L.; Liu, H.-B.; Lai, S.-W.; Che, C.-M.; Li, Y.-L. *Chem.—Eur. J.* **2012**, *18*, 4782−4790. (o) White, N. G.; Beer, P. D. *Beilstein J. Org. Chem.* **2012**, *8*, 246−252. (p) Yang, S.-T.; Liao, D.-J.; Chen, S.-J.; Hu, C.-H.; Wu, A.-T. *Analyst* **2012**, *137*, 1553−1555. (q) Yu, G.; Zhang, Z.; Han, C.; Xue, M.; Zhou, Q.; Huang, F. *Chem. Commun.* **2012**, *48*, 2958−2960.
(32) Triazole CH···anion interactions from 2013 to 2014: (a) Beckendorf, S.; Asmus, S.; Muck-Lichtenfeld, C.; Mancheno, O. G. *Chem.—Eur. J.* **2013**, *19*, 1581−1585. (b) Cai, J. J.; Hay, B. P.; Young, N. J.; Yang, X. P.; Sessler, J. L. *Chem. Sci.* **2013**, *4*, 1560−1567. (c) Cao, Q. Y.; Han, Y. M.; Wang, H. M.; Xie, Y. *Dyes Pigm.* **2013**, *99*, 798−802. (d) Cao, Q. Y.; Wang, Z. C.; Li, M.; Liu, J. H. *Tetrahedron Lett.* **2013**, *54*, 3933−3936. (e) Garcia, F.; Arago, J.; Viruela, R.; Orti, E.; Sanchez, L. *Org. Biomol. Chem.* **2013**, *11*, 765−772. (f) Gonzalez, M. D.; Oton, F.; Espinosa, A.; Tarraga, A.; Molina, P. *Chem. Commun.* **2013**, *49*, 9633−9635. (g) Merckx, T.; Verwilst, P.; Dehaen, W. *Tetrahedron Lett.* **2013**, *54*, 4237−4240. (h) Pfukwa, R.; Kouwer, P. H. J.; Rowan, A. E.; Klumperman, B. *Angew. Chem., Int. Ed.* **2013**, *52*, 11040−11044. (i) Romero, T.; Orenes, R. A.; Tarraga, A.; Molina, P. *Organometallics* **2013**, *32*, 5740−5753. (j) White, N. G.; Beer, P. D. *Org. Biomol. Chem.* **2013**, *11*, 1326−1333. (k) White, N. G.; Costa, P. J.; Carvalho, S.; Felix, V.; Beer, P. D. *Chem.—Eur. J.* **2013**, *19*, 17751−17765. (l) Cao, L.; Jiang, R. S.; Zhu, Y. L.; Wang, X. L.; Li, Y. J.; Li, Y. L. *Eur. J. Org. Chem.* **2014**, 2687−2693. (m) Gonzalez, M. D.; Oton, F.; Orenes, R. A.; Espinosa, A.; Tarraga, A.; Molina, P. *Organometallics* **2014**, *33*, 2837−2852. (n) Karagollu, O.; Gorur, M.; Gode, F.; Sennik, B.; Yilmaz, F. *Sens. Actuators, B* **2014**, *193*, 788−798. (o) Schulze, B.; Schubert, U. S. *Chem. Soc. Rev.* **2014**, *43*, 2522−2571. (p) Shang, J.; Gallagher, N. M.; Bie, F. S.; Li, Q. L.; Che, Y. K.; Wang, Y.; Jiang, H. *J. Org. Chem.* **2014**, *79*, 5134−5144. (q) Wang, L. Y.; Fang, G. P.; Ye, D. C.; Cao, D. R. *Sens. Actuators, B* **2014**, *195*, 572−580.
(33) (a) Khan, A.; Kaiser, C.; Hecht, S. *Angew. Chem., Int. Ed.* **2006**, *45*, 1878−1881. (b) Khan, A.; Hecht, S. *Chem.—Eur. J.* **2006**, *12*, 4764−4774. (c) Yu, Z.; Hecht, S. *Angew. Chem., Int. Ed.* **2011**, *50*, 1640−1643. (d) Yu, Z.; Hecht, S. *Chem.—Eur. J.* **2012**, *18*, 10519−10524. (e) Yu, Z.; Weidner, S.; Risse, T.; Hecht, S. *Chem. Sci.* **2013**, *4*, 4156−4167. (f) Yu, Z.; Hecht, S. *Angew. Chem., Int. Ed.* **2013**, *52*, 13740−13744.
(34) (a) Tie, C.; Callucci, J. C.; Parquette, J. R. *J. Am. Chem. Soc.* **2006**, *128*, 1162−1171. (b) King, E. D.; Tao, P.; Sanan, T. T.; Hadad, C. M.; Parquette, J. R. *Org. Lett.* **2008**, *10*, 1671−1674.
(35) Boyle, M. M.; Smaldone, R. A.; Whalley, A. C.; Ambrogio, M. W.; Botros, Y. Y.; Stoddart, J. F. *Chem. Sci.* **2011**, *2*, 204−210.
(36) Kume, S.; Murata, M.; Ozeki, T.; Nishihara, H. *J. Am. Chem. Soc.* **2004**, *127*, 490−491.
(37) (a) Barfield, M.; Gearhart, H. L. *J. Am. Chem. Soc.* **1973**, *95*, 641−643. (b) Jones, I. G.; Jones, W.; North, M. *J. Org. Chem.* **1998**, *63*, 1505−1513. (c) Loughlin, W. A.; Tyndall, J. D. A.; Glenn, M. P.; Fairlie, D. P. *Chem. Rev.* **2004**, *104*, 6085−6117.
(38) Albert, J. S.; Hamilton, A. D. *Biochemistry* **1995**, *34*, 984−990.
(39) Suk, J.-m.; Naidu, V. R.; Liu, X.; Lah, M. S.; Jeong, K.-S. *J. Am. Chem. Soc.* **2011**, *133*, 13938−13941.
(40) Li, Y.; Huffman, J. C.; Flood, A. H. *Chem. Commun.* **2007**, 2692−2694.
(41) Bryantsev, V. S.; Hay, B. P. *Org. Lett.* **2005**, *7*, 5031−5034.

(42) Zhang, J.; Moore, J. S. *J. Am. Chem. Soc.* **1992**, *114*, 9701−9702.
(43) (a) Sonogashira, K.; Tohda, Y.; Hagihara, N. *Tetrahedron Lett.* **1975**, *16*, 4467−4470. (b) Negishi, E.; Anastasia, L. *Chem. Rev.* **2003**, *103*, 1979−2017.
(44) (a) Rostovtsev, V. V.; Green, L. G.; Fokin, V. V.; Sharpless, K. B. *Angew. Chem., Int. Ed.* **2002**, *41*, 2596−2599. (b) Tornøe, C. W.; Christensen, C.; Meldal, M. *J. Org. Chem.* **2002**, *67*, 3057−3064.
(45) Latyshev, G. V.; Baranov, M. S.; Kazantsev, A. V.; Averin, A. D.; Lukashev, N. V.; Beletskaya, I. P. *Synthesis* **2009**, 2605−2615.
(46) Tsuji, M. *J. Org. Chem.* **2003**, *68*, 9589−9597.
(47) Zhang, C.; Jiao, N. *Angew. Chem., Int. Ed.* **2010**, *49*, 6174−6177.
(48) (a) Sadovski, O.; Beharry, A. A.; Zhang, F.; Woolley, G. A. *Angew. Chem., Int. Ed.* **2009**, *48*, 1484−1486. (b) Beharry, A. A.; Sadovski, O.; Woolley, G. A. *J. Am. Chem. Soc.* **2011**, *133*, 19684−19687.
(49) Stone, M. T.; Heemstra, J. M.; Moore, J. S. *Acc. Chem. Res.* **2006**, *39*, 11−20.
(50) Lee, S.; Chen, C.-H.; Flood, A. H. *Nat. Chem.* **2013**, *5*, 704−710.
(51) It is known that *ortho* and *para* substitutions on azobenzene give rise to large changes in its electronic structure and photoisomerization properties. However, *meta* substitution of azobenzene, as is present in **F1**, **F2**, and **F3**, has relatively minor effects. See: Ruslim, C.; Ichimura, K. *J. Mater. Chem.* **2000**, *10*, 2704−2707. Dokić, J.; Gothe, M.; Wirth, J.; Peters, M. V.; Schwarz, J.; Hecht, S.; Saalfrank, P. *J. Phys. Chem. A* **2009**, *113*, 6763−6773.
(52) Koepf, E. K.; Petrassi, H. M.; Sudol, M.; Kelly, J. W. *Protein Sci.* **1999**, *8*, 841−853.
(53) (a) Sonnichsen, F. D.; Van Eyk, J. E.; Hodges, R. S.; Sykes, B. D. *Biochemistry* **1992**, *31*, 8790−8798. (b) Jasanoff, A.; Fersht, A. R. *Biochemistry* **1994**, *33*, 2129−2135.
(54) Vander Griend, D. A.; Bediako, D. K.; DeVries, M. J.; DeJong, N. A.; Heeringa, L. P. *Inorg. Chem.* **2007**, *47*, 656−662.
(55) (a) Yamamoto, J.; Kunikata, H.; Umezu, M. *Nippon Kagaku Kaishi* **1983**, 78−81. (b) Baik, W.; Kim, D. I.; Koo, S.; Rhee, J. U.; Shin, S. H.; Kim, B. H. *Tetrahedron Lett.* **1997**, *38*, 845−848.
(56) Zhang, C.; Jiao, N. *Angew. Chem., Int. Ed.* **2010**, *49*, 6174−6177.